

Modification of relativistic beam fields under the influence of external conducting and ferromagnetic flat boundaries

B. B. Levchenko*

D. V. Skobeltsyn Institute of Nuclear Physics, M. V. Lomonosov Moscow State University, 119991 Moscow, Russian Federation

*E-mail: levchen@mail.desy.de

Received March 30, 2019; Revised October 2, 2019; Accepted October 17, 2019; Published January 23, 2020

.....
We derive analytical expressions for external fields of a relativistic bunch of charged particles with a circular and an elliptical cross section under different boundary conditions and interaction of the fields with an accelerator structural elements. The particle density in the bunch is assumed to be uniform as well as non-uniform. At distances far apart from the bunch, in free space the field reduces to the relativistic modified Coulomb form for a pointlike charge and at small distances the expressions reproduce the external fields of a continuous beam. In an ultra-relativistic limit the longitudinal components of the internal and external electric fields of the bunch are strongly suppressed by the Lorentz factor. If the bunch is surrounded by conducting surfaces, the bunch self-fields are modified. Image fields generated by a bunch between two parallel conducting plates are studied in detail. Exact summation of the electric, E_y , and magnetic, B_x , image field components allows the infinite series to be represented in terms of elementary trigonometric functions. The new expressions for modified fields are applied to study image forces acting on the bunch constituents and the bunch as a whole. The coherent and incoherent tune shifts for an arbitrary bunch displacement from the midplane are calculated in the framework of an improved linear theory, for both infinite and finite parallel flat surfaces. Moreover, the developed method allows us to generalize the Laslett image coefficients ϵ_1 , ϵ_2 , ξ_1 , ξ_2 to the case of an arbitrary bunch offset and reveal relationships between these coefficients. Appendix C provides a brief historical background of the development of the method of electrical images.
.....

Subject Index G10

1. Introduction

In an accelerator, the charged beam is influenced by the environment matter (a beam pipe, accelerator gaps, magnets, collimators, etc.), and a high-intensity bunch of particles induces surface charges or currents into this environment. This modifies the electric and magnetic fields around the bunch. There is a relatively simple method to account for the effect of the environment by introducing image charges and currents. The mathematical technique of electrical images was developed by W. Thomson (Lord Kelvin) [1–3]. The method of images has found application in various branches of physics, in particular, in hydrodynamics [4–6]. Appendix C provides a brief historical background on the subject¹.

¹ 20th century textbooks on classical electrodynamics do not specify the author of the method of electrical images.

Over fifty years ago Laslett [7,8] analyzed the influence of the transverse space-charge phenomena, due to image forces, on the instability of the coherent transverse motion of an intense beam. Methods of image field summation are described in his paper [7], which presented some field coefficients calculated for infinite parallel plate vacuum chambers, magnet poles, and vacuum chambers with elliptical cross sections and variable aspect ratios. The resulting image fields were calculated only in the linear approximation and depend linearly on the deviations \bar{y} and y of the bunch center and the position of a test particle, respectively, from the axis (see Fig. 4). They act therefore like a quadrupole causing a coherent tune shift. The approximation used is incorrect if the field observation point y is located far from the bunch or if the bunch center \bar{y} is close to a conducting wall.

In the present paper we consider this classical problem summation of fields of images once again for a very simple geometry, namely, an ultra-relativistic bunch moving between infinitely wide parallel perfectly conducting plates. The problem is far from being purely academic. In applications, in particular, in the study of dynamics of photoelectrons in the beam transport system [9] and the electron cloud effect intensified by electron field emission in the flat collimator [10], it is important to know the distribution of electromagnetic fields not only in the vicinity of the bunch, but in the whole collimator gap. We have not found publications with attempts to sum up the series (34) (see Sect. 4) in an approximation beyond the linear one. In Sects. 4 and 5 we present exact 1D solutions of the problem for electric and magnetic image fields. The preliminary results were presented in Ref. [11]. 1D solutions are canonically used in the calculation of tune shifts².

Before we solve the problem formulated above, in Sect. 2 we first derive expressions for the external electric and magnetic fields generated by a cylindrical and an elliptical bunch of charged particles. The task is specified as follows.

The external radial electric field \vec{E}_r and azimuthal magnetic induction \vec{B}_ϕ for a round unbunched relativistic beam of radius a and a uniform charge density are described by [12–14]

$$E_r = \kappa \frac{2q\lambda}{r}, \quad (1)$$

$$B_\phi = \frac{\mu_0}{4\pi} \frac{2q\lambda}{r} c\beta, \quad (2)$$

where $\kappa = 1/4\pi\epsilon_0$, λ is the linear beam density, q is the charge, $\beta = v/c$ is a normalized velocity of the beam constituents, and c the velocity of light³. In many applications, Eqs. (1) and (2) are used to describe fields of an individual bunch too. However, in the form (1), (2) the bunch fields do not depend on the bunch energy and at large distances do not follow the Coulomb asymptotic. This contrasts sharply with the fields produced (at $t = 0$) by a rapidly moving single charge q :

$$\vec{E} = \kappa \frac{q\gamma}{r^2} \left[\frac{1 - \beta^2}{1 - \beta^2 \sin^2 \theta} \right]^{3/2} \frac{\vec{r}}{r}, \quad c\vec{B} \sim \vec{\beta} \times \vec{E}, \quad (3)$$

where θ is the angle that the vector \vec{r} makes with the z -axis. Along the direction of motion the electric field becomes weaker in γ^2 times, while in the transverse direction the electric field is enhanced by

² Exact 2D solutions by the method of images and other applications will be presented elsewhere.

³ In Ref. [13], the azimuthal component B_ϕ , Eqs. (18.51)–(18.52), includes the minus sign, in contradiction to Eq. (18.28) and the expression of cylindrical coordinates of a vector field by Cartesian coordinates (Ref. [15], p. 630): $B_\phi = -B_x \sin \phi + B_y \cos \phi$.

the factor γ :

$$E_r = \kappa \frac{q\gamma}{r^2}. \quad (4)$$

Here, γ denotes the particle Lorentz factor.

This paper is organized as follows. In the next section, we demonstrate how, when summing up the elementary electromagnetic fields generated by charged relativistic particles, effective external beam fields are formed. We derive expressions for the transverse and longitudinal components of the bunch electric field, where the defects indicated above are rectified, and find the conditions at which the bunch fields are represented by Eqs. (1) and (2). Here we consider bunches shaped as a cylinder with a circular and an elliptical cross section. In Sect. 3 we discuss fields generated by a bunch with an arbitrary linear particle density and make a statement that in the ultra-relativistic limit $\gamma \rightarrow \infty$ the electric field takes a universal form.

Sections 4 and 5 are devoted to the problem of finding exact analytic expressions for the electric and magnet fields generated by a bunch moving between infinitely wide parallel conducting plates and magnet poles.

In Sect. 6 we discuss image forces acting on the bunch constituents and the bunch as a whole and calculate in the framework of an improved linear approximation the coherent and incoherent tune shifts for an arbitrary bunch displacement from the midplane. In Sect. 6.3, a practical example is considered as gradients of image fields in a finite-size collimator affecting the betatron frequency of the beam. Conclusions are drawn in Sect. 7. Here we also compare results obtained by different authors with the use of various techniques. Detailed derivations of the obtained results are placed in Appendixes A and B.

2. Self-fields of a charged cylinder with an elliptical cross section

Let us consider a bunch of charged particles uniformly distributed with a density ρ within a cylinder of length L and an elliptical cross section. The ellipsoid semi-axes in the x - y plane are a and b and the coordinate z -axis is along the bunch axis. Suppose that the bunch is moving along the z -axis with a relativistic velocity $\vec{v} = c\vec{\beta}$.

To compute the radial electric field of such a rapidly moving bunch, we have to sum up fields of the type (3), generated by the bunch constituents. In this way we get [16]

$$E_{\perp}(r, \xi, z) = \kappa\rho\gamma[zI_1 + (L-z)I_2] \quad (5)$$

with

$$I_1 = \iint \frac{[r - \sigma \cos(\xi - \phi)] \sigma d\sigma d\phi}{[r^2 + \sigma^2 - 2r\sigma \cos(\xi - \phi)][\gamma^2 z^2 + r^2 + \sigma^2 - 2r\sigma \cos(\xi - \phi)]^{1/2}} \quad (6)$$

$$I_2 = \iint \frac{[r - \sigma \cos(\xi - \phi)] \sigma d\sigma d\phi}{[r^2 + \sigma^2 - 2r\sigma \cos(\xi - \phi)][\gamma^2(L-z)^2 + r^2 + \sigma^2 - 2r\sigma \cos(\xi - \phi)]^{1/2}} \quad (7)$$

where σ is the distance in the x - y plane from the z -axis to the elementary charged volume and

$$0 < \sigma \leq \Sigma(\phi) = \frac{b}{\sqrt{1 - e^2 \cos^2 \phi}}, \quad 0 < \phi < 2\pi, \quad (8)$$

where $e = \sqrt{1 - b^2/a^2}$ is the eccentricity of an ellipse and $a > b$. Equation (5) represents the radial electric field at instant $t = 0$ as observed at a distance r from the bunch axis, at an angle ξ relative to the x -axis and at a distance z from the bunch tail.

In Ref. [16] integrals I_1 and I_2 were estimated only numerically, because the integrands were taken as they are. However, the integrands are easy to simplify if the bunch is ultra-relativistic, $\gamma \gg 1$, and we would now like to calculate the field in the vicinity of the bunch but at distances much larger than the bunch radius, $r \gg a$.

To simplify this, we make use of the notations

$$A = \sigma/r, \quad B = A \cos(\xi - \phi), \quad Y = A^2 - 2B,$$

$$C_1 = \left[1 + \gamma^2 z^2/r^2\right]^{-1}, \quad X = C_1 \cdot Y$$

and the integrand of I_1 can be written as

$$(r^2 + \gamma^2 z^2)^{-1/2} A(1 - B)(1 + Y)^{-1}(1 + X)^{-1/2}. \tag{9}$$

Now we expand the above expression in a power series by using A as a small parameter and keeping only terms up to the power A^4 at each step.

2.1. Finite circular cylinder with a uniform particle density

For a bunch shaped as a circular cylinder, $a = b$, we may set $\xi = 0$. Due to the fact that

$$\int_0^{2\pi} \cos^{2k+1} \phi \, d\phi = 0, \tag{10}$$

all odd powers of B vanish after integration over ϕ . This greatly simplifies the series generated from Eq. (9). After lengthy algebraic manipulations with Eq. (9), we get

$$(r^2 + \gamma^2 z^2)^{-1/2} A \left[1 - (1 + \frac{1}{2} C_1) A^2 + (2 + C_1 + \frac{3}{2} C_1^2) B^2 \right]. \tag{11}$$

Substituting this expression in Eq. (6), one gets

$$I_1 = \frac{\pi a^2}{r \sqrt{r^2 + \gamma^2 z^2}} \left(1 + \frac{3}{8} C_1^2 \frac{a^2}{r^2} \right). \tag{12}$$

By changing z^2 to $(L - z)^2$ in Eq. (12), we obtain for I_2 the following result:

$$I_2 = \frac{\pi a^2}{r \sqrt{r^2 + \gamma^2 (L - z)^2}} \left(1 + \frac{3}{8} C_2^2 \frac{a^2}{r^2} \right), \tag{13}$$

where $C_2 = \left[1 + \gamma^2 (L - z)^2/r^2\right]^{-1}$. Notice that for particles uniformly distributed in the bunch volume, $\rho = qN_b/\pi a^2 n_b L = q\lambda/\pi a^2$, where N_b is the total number of particles in the beam, n_b the number of bunches, and λ the linear particle density. Substituting Eqs. (12)–(13) in Eq. (5), we finally arrive at

$$E_{\perp}(r, z) = \kappa \frac{q\lambda\gamma}{r} \left[\frac{z}{\sqrt{r^2 + \gamma^2 z^2}} \left(1 + \frac{3}{8} \frac{a^2}{r^2} C_1^2 \right) + \frac{L - z}{\sqrt{r^2 + \gamma^2 (L - z)^2}} \left(1 + \frac{3}{8} \frac{a^2}{r^2} C_2^2 \right) \right]. \tag{14}$$

This equation describes the transverse component of the electric field produced by a rapidly moving circular bunch. For $\gamma \gg 1$ the correction factors C_1 and C_2 can be neglected. In that case at the

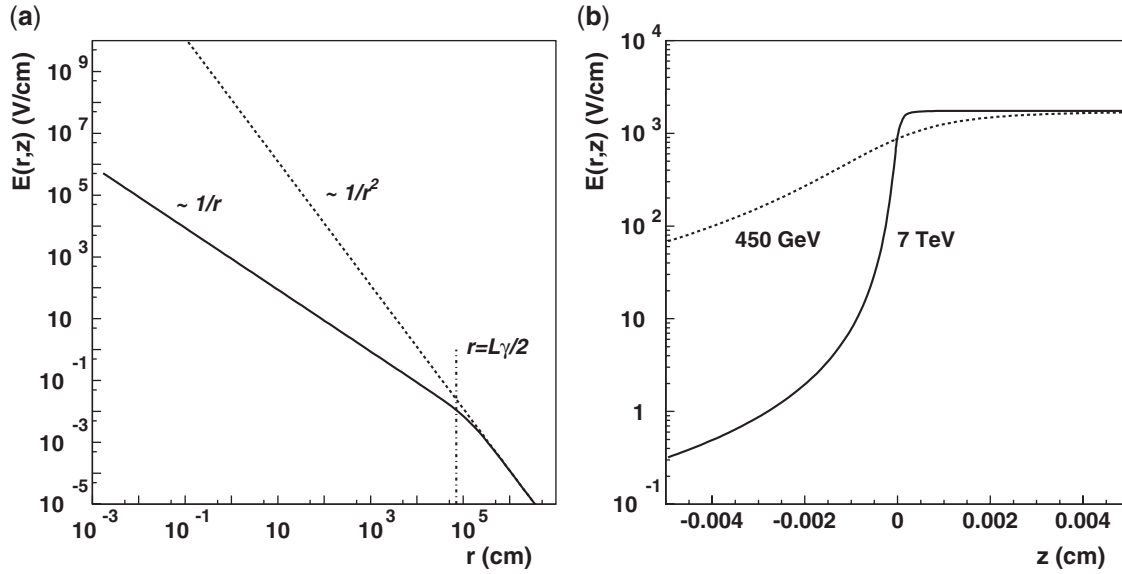


Fig. 1. (a) The transverse profile of the electric field generated by a relativistic bunch of a circular cross section. The vertical dash-dotted line indicates the crossover point of the curve (4) and (1). Here $L = \sqrt{2\pi}\sigma_z$ and σ_z denoting the r.m.s. bunch length. (b) The radial field variation with z near the bunch tail at fixed $r = 1.0$ cm. For comparison, the dashed line shows the field from a proton bunch at the energy 450 GeV. Calculations are performed with parameters corresponding to the LHC proton beam (see Table 1).

bunch surface, $r = a$, Eq. (14) exactly matches the equation for the internal field [16]. Therefore, the condition $r \gg a$ used to derive Eq. (14) can be weakened and Eq. (14) is valid in the region $r \geq a$.

The field of a relativistic bunch described by Eq. (14) has different behavior at distances far away from the bunch and for $r < L\gamma/2$. Figure 1(a) shows the radial field profile as follows from Eq. (14). The parameters of the bunch correspond to the nominal scenario of the LHC proton beam [17]. At very large distances, $r \gg L\gamma/2$, Eq. (14) reduces to the Coulomb form (4) with q replaced by qN_b/n_b . Calculations show that for a proton bunch at 7 TeV the Coulomb law is restored only at a distance of several kilometers from the bunch. On the other hand, for $r \ll L\gamma/2$, Eq. (14) simplifies to a form independent of the z -coordinate, which coincides with the external field (1) of a continuous beam with $\lambda = N_b/n_bL$.

The magnitude of the electric field varies drastically in the head and tail parts of the bunch. For instance, in a very narrow transition region beyond the bunch tail, $z < 0$, $|z| \ll r/\gamma$, the field strength decreases with z as follows:

$$E_{\perp}(r, z) \approx \kappa \frac{q\lambda}{r} \left[1 - \frac{r^2}{2\gamma^2(L-z)^2} \right]. \tag{15}$$

However, at larger $|z|$, the suppression of the radial field by the Lorentz factor becomes dominant:

$$E_{\perp}(r, z) \approx \kappa \frac{q\lambda r}{2\gamma^2} \frac{L(L-2z)}{z^2(L-z)^2}. \tag{16}$$

This is shown in Fig. 1(b). The field strength decreases to more than three orders of magnitude at a distance of $4 \mu\text{m}$ beyond the bunch. One finds from Eq. (14) that at $z \geq L$ the field magnitude tends to zero in a similar way.

The longitudinal part of the electric field reaches the maximum value on the bunch axis, so that on axis the longitudinal electric field is given by [16]

$$E_z(0, z) = \kappa \frac{2\pi\rho}{\gamma} \{ \sqrt{a^2 + \gamma^2(L-z)^2} - \sqrt{a^2 + \gamma^2z^2} + \gamma|z| - \gamma|L-z| \}. \quad (17)$$

At $\gamma \gg 1$, the field magnitude outside the bunch is given by

$$E_z(0, z) = \kappa \frac{q\lambda}{\gamma^2} \left[\frac{1}{|L-z|} - \frac{1}{|z|} \right]. \quad (18)$$

Equation (18) shows that the longitudinal field is independent of the bunch radius and strongly suppressed along the line of motion of the bunch.

The main result of this consideration is that due to features (16) and (18), the space-time distribution of the electric field around an ultra-relativistic circular bunch with a uniform particle density is well approximated by a step-like form:

$$E(r, z, t) = \kappa \frac{2q\lambda}{r} \left[\theta(z - \beta ct) - \theta(z - \beta ct - L) \right]. \quad (19)$$

Similarly, we can show that the azimuthal magnetic induction of the bunch is

$$B_\phi(r, z, t) = \frac{\mu_0}{4\pi} \frac{\beta c}{\kappa} E_\perp(r, z, t). \quad (20)$$

2.2. Finite elliptical cylinder with a uniform particle density

Let us now consider a bunch shaped as an elliptical cylinder. We make use of the same notations as in the previous subsection. In the ultra-relativistic scenario, the correction factors C_1 and C_2 should be neglected from the beginning. By expanding the integrand of I_1 in a power series as above, we get

$$\begin{aligned} & (r^2 + \gamma^2z^2)^{-1/2} \left\{ \sum_{k=0}^{k_{\max}} A^{2k+1} \cos[2k(\xi - \phi)] \right. \\ & + A^2 \cos(\xi - \phi) [1 - A^2(1 - \cos[2(\xi - \phi)]) + A^4(1 - 2\cos[2(\xi - \phi)] + 2\cos[4(\xi - \phi)]) \\ & \left. - A^6(1 - 2\cos[2(\xi - \phi)] + 2\cos[4(\xi - \phi)] - 2\cos[6(\xi - \phi)]) + \dots \right\}. \quad (21) \end{aligned}$$

It can be proven that for an even function $f_n(\phi)$

$$\int_0^{2\pi} d\phi \cos^{2k+1}(\xi - \phi) \int_0^{\Sigma(\phi)} d\sigma A^n = \frac{b^{n+1}}{(n+1)r^n} \int_0^{2\pi} f_n(\phi) \cos^{2k+1}(\xi - \phi) d\phi = 0, \quad (22)$$

where $k = 0, 1, 2, \dots$. In our consideration

$$f_n(\phi) = (1 - e^2 \cos^2 \phi)^{-(n+1)/2}. \quad (23)$$

The integral (6) now can be solved with respect to σ and ϕ by direct substitution of Eq. (21) and the use of Eq. (22):

$$I_1 = \frac{\pi ab}{r\sqrt{r^2 + \gamma^2z^2}} \frac{\sqrt{1 - e^2}}{\pi} \sum_{k=0}^{k_{\max}} \frac{b^{2k}}{(2k+2)r^{2k}} \cdot D_k \cdot \cos(2k\xi). \quad (24)$$

The condition (22) causes all even terms in A to vanish. Here,

$$D_k = \int_0^{2\pi} \frac{\cos(2k\phi) d\phi}{(1 - e^2 \cos^2 \phi)^{k+1}} = d_k \cdot \frac{\pi e^{2k}}{(1 - e^2)^{k+1/2}}, \tag{25}$$

with numerical coefficients $d_k = (2, 1, 3/4, 5/8, 35/64, 63/128, 231/524, 429/1024, \dots)$. By changing z^2 to $(L - z)^2$ in Eq. (24), one finds I_2 too.

For particles uniformly distributed in the elliptical bunch volume, $\rho = q\lambda/\pi ab$ with $\lambda = N_b/n_b L$ the linear particle density. Substituting equations for I_1 and I_2 in Eq. (5), we finally arrive at

$$E_{\perp}(r, z) = \kappa \frac{q\lambda\gamma}{r} \left(\frac{z}{\sqrt{r^2 + \gamma^2 z^2}} + \frac{L - z}{\sqrt{r^2 + \gamma^2 (L - z)^2}} \right) \left[1 + \frac{1}{4} \left(\frac{ae}{r} \right)^2 \cos(2\xi) + \frac{1}{8} \left(\frac{ae}{r} \right)^4 \cos(4\xi) + \frac{5}{64} \left(\frac{ae}{r} \right)^6 \cos(6\xi) + \frac{7}{128} \left(\frac{ae}{r} \right)^8 \cos(8\xi) + \dots \right]. \tag{26}$$

This equation describes the transverse component of the electric field produced by a rapidly moving elliptical bunch of length L . The transverse part is modulated by an angular factor that takes into account the ellipticity of the bunch. The dimensions of the ellipse enters only via the ratio ae/r .

The arguments used in deriving Eq. (19) are also applicable here. The electric field of an ultra-relativistic elliptical bunch is therefore well approximated by a step-like form:

$$E(r, z, \xi, t) = \kappa \frac{2q\lambda}{r} \left[\theta(z - \beta ct) - \theta(z - \beta ct - L) \right] \left[1 + \frac{1}{4} \left(\frac{ae}{r} \right)^2 \cos(2\xi) + \frac{1}{8} \left(\frac{ae}{r} \right)^4 \cos(4\xi) + \frac{5}{64} \left(\frac{ae}{r} \right)^6 \cos(6\xi) + \frac{7}{128} \left(\frac{ae}{r} \right)^8 \cos(8\xi) + \dots \right]. \tag{27}$$

The representation (27) with such ‘‘separation of variables’’ (r, ξ) is useful in an analytic calculation, including a differentiation and an integration. The number of terms, k_{\max} , in Eqs. (24), (27) to be taken into account depends on the required precision.

The approximate formula (27) can now be contrasted with an exact expression of the electric field for a uniformly charged elliptical beam. There is a compact formula [18,19] in the complex (x, y) plane, $z = x + iy$, in the term of the ‘‘complex electric field’’:

$$E(z) \equiv E_x(z) + iE_y(z) = \frac{4\kappa q\lambda}{a^2 - b^2} (\bar{z} - \sqrt{\bar{z}^2 - a^2 + b^2}). \tag{28}$$

However, in the real components the formula is more complicated. Outside the beam, the x -component of the field is

$$E_x = \frac{4\kappa q\lambda}{(ae)^2} \left\{ x - \frac{\text{sign}(x)}{\sqrt{2}} \left[u + \sqrt{u^2 + (2xy)^2} \right]^{1/2} \right\}, \tag{29}$$

while the y -component can be obtained from this by exchanging $x \leftrightarrow y$ and $a \leftrightarrow b$. Here $u = x^2 - y^2 - (ae)^2$. Thus,

$$E_{\perp}(r, \xi) = \sqrt{E_x^2(r, \xi) + E_y^2(r, \xi)} \tag{30}$$

with $x = r \cos \xi$ and $y = r \sin \xi$.

We are now in a position to evaluate the number of terms in Eq. (27) that need to be taken into account in order to get the precision, say, to better than 5%, if compared with the exact formula (30). Figure 2(a) shows the variation of the ratio of Eq. (27) to Eq. (30) with the azimuthal angle ξ in

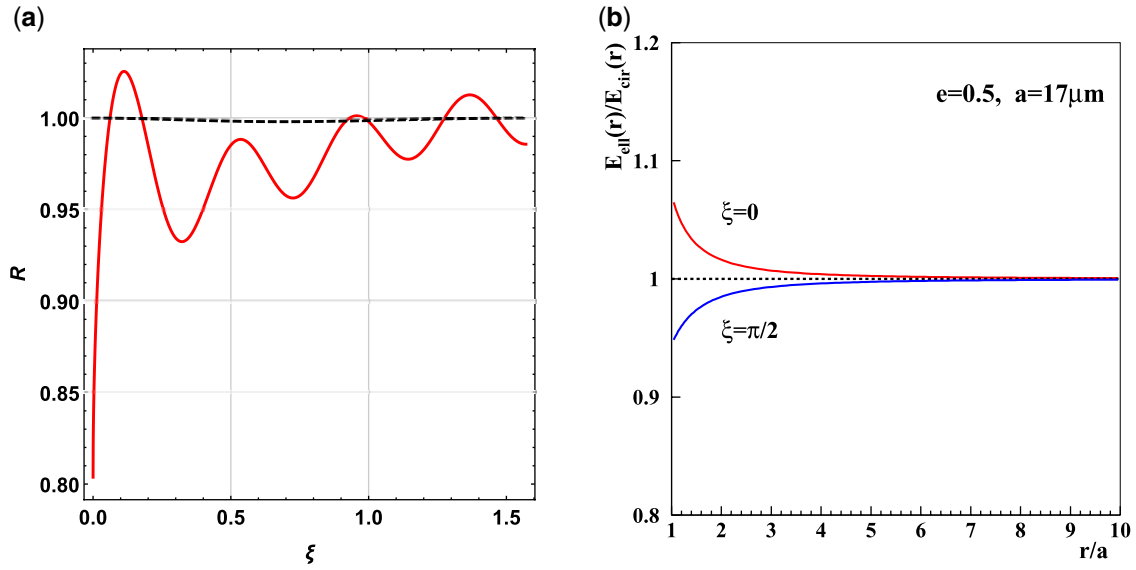


Fig. 2. (a) The ratio of electrical field (27) to electrical field (30) as a function of ξ in the first quadrant. The calculation is done at $r/ae = 1$ (full curve) and $r/ae = 2$ (dashed curve) with $k_{\max} = 7$ (see Eq. (24)). (b) The ratio of the electrical field (27) created by an elliptical bunch ($e = 0.5$ and $a = 17 \mu\text{m}$) to the electrical field (19) created by a circular bunch ($a = 17 \mu\text{m}$) as a function of the radial distance at the azimuthal angle $\xi = 0$ and $\xi = \pi/2$.

the first quadrant. We observe that at $r/ae = 1$ (full curve) the desired precision is almost reached at $k_{\max} = 7$, except for the area near $\xi = 0$. In this area, it is necessary to account for terms with $k_{\max} > 7$ to achieve the required precision. At the same time, at $r/ae = 2$ and $k_{\max} = 7$ (dashed curve), the accuracy is better than 1% in the entire area of ξ .

The azimuthal field variation is essential only at $r \sim a$. For instance, for a flat beam and at $r = a$, the field is concentrated at $\xi = 0$ and π . However, at larger r (say, $r > 5a$) the angular dependence vanishes rapidly and the electric field of an ultra-relativistic elliptical bunch converges to the universal form (19). The last statement is illustrated by Fig. 2(b).

3. Universality of a bunch external fields

The uniform particle density considered in the last section is an idealization. In reality, the linear particle density, $\lambda(z)$, varies considerably along the bunch. As an example, Fig. 3(a) shows the current profile of electron bunches in the XFEL accelerator [20]. Electrons of energy 17.5 GeV form bunches with a charge of 1 nC and a peak current of 5 kA. The current distribution is well fitted by a sum of two Gaussian distributions and a polynomial pedestal. Certainly, these bunches are ultra-relativistic since $\gamma = 3.2 \times 10^4$. Now the question arises of how to calculate the electric field of the bunch for a given distribution of the current density $J(z) = q\beta c\lambda(z)$.

We will now argue that in the asymptotic limit $\gamma \rightarrow \infty$ the problem has a simple solution.

The main conclusion that we can draw from the previous consideration is that at a distance of several bunch radii, the electric field of the bunch is independent of the transverse geometry of the bunch. Without loss of generality let us consider again a bunch with a circular cross section. The distribution $J(z)$ can be well approximated by a histogram $J_i = q\beta c\lambda_i$, as shown in Fig. 3(b). Let us imagine that the bunch is a set of layers with a thickness of Δz_i . Suppose that in the transverse direction particles are distributed uniformly and the linear particle density varies from one layer

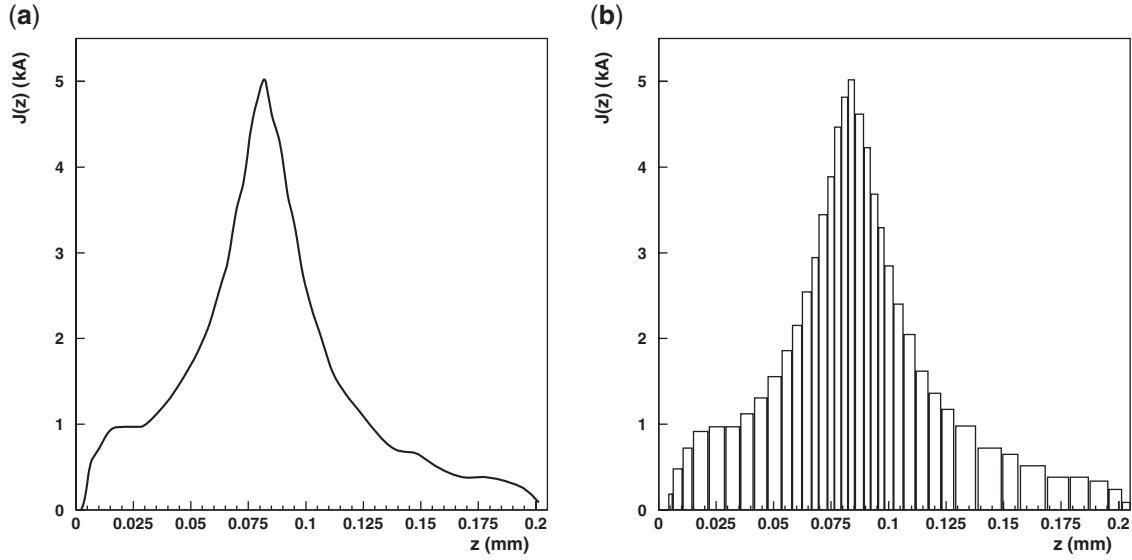


Fig. 3. (a) The current profile of an electron bunch in the XFEL accelerator [20] and (b) its representation as a histogram with a variable bin size Δz_i .

to the next in accordance with λ_i . Thus, each layer is a cylinder with a uniform particle density acting as an independent field source. The complete field of the bunch is a sum of elementary field sources (19):

$$E(r, z) = \kappa \frac{2q}{r} \sum_i \left[\theta(z - z_i) - \theta(z - z_i - \Delta z_i) \right] \lambda_i = \kappa \frac{2q}{r} \lambda(z, t). \quad (31)$$

Here we have used

$$\lim_{\Delta z_i \rightarrow 0} \frac{\theta(z - z_i) - \theta(z - z_i - \Delta z_i)}{\Delta z_i} \Delta z_i = \delta(z - z_i) dz_i,$$

and the sum is replaced by an integration. We obtain the same result (31) even if we consider a bunch with a variable cross section and a uniform transverse density in each slice Δz_i .

We conclude with a statement that summarizes the obtained results:

THEOREM 1 *In the ultra-relativistic limit, $\gamma \rightarrow \infty$, the external electric field of a bunch with a linear particle density $\lambda(z)$ is governed by the universal law*

$$E(r, z, t) = \kappa \frac{2q}{r} \lambda(z, t). \quad (32)$$

It is instructive to compare the strength of the electric field created by a cylindrical bunch with a uniform particle density $\lambda_U = N/L$ and a bunch with the Gaussian particle distribution $\lambda_G(z)$. The ratio of the fields is

$$\frac{E_G}{E_U} = \frac{\lambda_G(z)}{\lambda_U} = \frac{L}{L_{\text{eff}}} \exp\left(-\frac{z^2}{2\sigma_z^2}\right). \quad (33)$$

Thus, if L is equal to the effective length of the Gaussian bunch $L_{\text{eff}} = \sqrt{2\pi}\sigma_z$, the field strengths in both cases are equal at the maximum of $\lambda_G(z)$. Note, however, that in a more general case, as in Fig. 3,

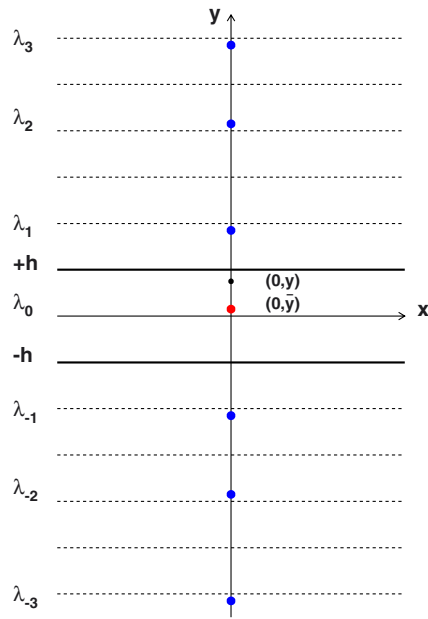


Fig. 4. The electric field seen by a particle at location y on the y -axis is generated by the direct source-charge λ_0 at \bar{y} and the successive image charges $\lambda_{\pm i}$ at locations $d_{\pm k}$ and $d_{\pm m}$ (see explanation in the text).

that conclusion is not correct, even if $L = L_{\text{eff}}$. For instance, with the parameters of an XFEL bunch [20], one finds $L_{\text{eff}} = 0.217$ mm and at the maximum of the current density $E_{\text{XFEL}}/E_U = 3.63$.

So far, we have considered fields in free space. In an accelerator, the charged beam is influenced by an environment and a high-intensity bunch induces surface charges or currents into this environment. This modifies the electric and magnetic fields around the bunch. There is a relatively simple method to account for the effect of the environment by introducing image charges and currents.

4. Fields from image charges

“Definition of an electrical image. An electrical image is an electrified point or system of points on one side of a surface which would produce on the other side of that surface the same electrical action which the actual electrification of that surface really does produce” [21].

Following Laslett [7,8], we consider a relativistic bunch between infinitely wide conducting plates placed at $y = h$ and $y = -h$. Suppose that the constituents of the bunch are positively charged. For full generality, let the bunch be displaced by $(0, \bar{y}, 0)$ from the midplane $(x, 0, z)$, and the observation point of the field be at $(0, y, 0)$ between conducting parallel plates. The boundary condition for the electric field on perfectly conducting plates is $E_z(\pm h) = 0$ and is satisfied if the image charges change sign from image to image.

The electric field seen by a particle at location y on the y -axis is generated by the direct source-charge λ_0 and the successive image charges $\lambda_{\pm i}$ [14,22], as shown in Fig. 4. For instance, the image charges λ_1 and λ_{-1} are generated by λ_0 due to reflection in plates $+h$ and $-h$, respectively. The image charges λ_2 and λ_{-2} are generated by λ_{-1} and λ_1 due to reflection in plates $+h$ and $-h$, respectively, and so on. With the help of Fig. 4, one can easily calculate the distance between the image charge position and the observation point. So, for odd images, $k = 1, 3, 5, \dots$, the distances between $\lambda_{\pm k}$ and the point y are $d_{\pm k} = 2kh \mp y_1$. For even images, $m = 2, 4, 6, \dots$, the distances between $\lambda_{\pm m}$ and the point y are $d_{\pm m} = 2mh \mp y_2$. Here $y_1 = y + \bar{y}$ and $y_2 = y - \bar{y}$.

Suppose that the distance between plates is of the order $10a$. Thus, the electric field of each image is described by Eq. (32). To calculate the image electric field component $E_{y,\text{im}}(y)$ in front of the plate, we add the contributions from all image fields in the infinite series [7,8,13,22]:

$$E_{y,\text{im}}(y, \bar{y}, z, t) = 2\kappa q\lambda(z, t)[(2h - y_1)^{-1} - (2h + y_1)^{-1} - (4h - y_2)^{-1} + (4h + y_2)^{-1} + (6h - y_1)^{-1} - (6h + y_1)^{-1} - (8h - y_2)^{-1} + (8h + y_2)^{-1} + (10h - y_1)^{-1} - (10h + y_1)^{-1} - (12h - y_2)^{-1} + (12h + y_2)^{-1} + \dots]. \quad (34)$$

The representation (34) keeps the same form irrespective of the relative position of the bunch center and the observation point between plates, ($\bar{y} \geq 0, y \geq \bar{y}, y < \bar{y}$) or ($\bar{y} < 0, y \leq \bar{y}, y > \bar{y}$). These image fields must be added to the direct field of the bunch (32) to meet the boundary condition that the electric field enters conducting surfaces perpendicularly.

In the original paper [7] (see also Refs. [13,22]), the series (34) was summed up only in the linear approximation in y and \bar{y} :

$$E_{y,\text{im}}(y, \bar{y}) = \kappa \frac{4q\lambda}{h} \frac{\epsilon_1}{h} (y + 2\bar{y}). \quad (35)$$

The coefficient $\epsilon_1 = \pi^2/48$ is known as the Laslett coefficient (or form factor) for infinite parallel plate vacuum chambers. The approximation (35), widespread in textbooks and lectures, is, however, incorrect if the deviation of the bunch center from the axis is large ($\bar{y} \sim h$) or if the field observation point y is located far off the bunch. Therefore, below we present the exact solution of the problem.

In Appendix A it is proven that the exact summation of the series (34) gives

$$E_{y,\text{im}}(y, \bar{y}, z, t) = \kappa \frac{4q\lambda(z, t)}{h} \Lambda(\delta, \bar{\delta}), \quad (36)$$

where the electric image field structure function Λ depends only on scaled variables $\delta = y/h, \bar{\delta} = \bar{y}/h$ in the form

$$\Lambda(\delta, \bar{\delta}) = \frac{1}{2} \left[\frac{\pi}{2} \cdot \frac{\cos(\frac{\pi}{2}\bar{\delta})}{\sin(\frac{\pi}{2}\delta) - \sin(\frac{\pi}{2}\bar{\delta})} - \frac{1}{\delta - \bar{\delta}} \right]. \quad (37)$$

We have shown in Appendix A that the truncated linear approximation (36) recovers the part (35) derived by Laslett.

We shall now calculate values of $\Lambda(\delta, \bar{\delta})$ at several particular points along the y -axis.

$\delta = 1$: the observation point is located at the plate, $y = h$. In this case, the structure function depends only on the bunch center position between plates, $\bar{\delta}$. From Eq. (37) one gets

$$\Lambda(1, \bar{\delta}) = \frac{1}{2} \left[\frac{\pi}{2} \frac{1 + \sin(\frac{\pi}{2}\bar{\delta})}{\cos(\frac{\pi}{2}\bar{\delta})} - \frac{1}{1 - \bar{\delta}} \right]. \quad (38)$$

Equation (38) is singular at $\bar{\delta} \rightarrow 1$ and shows that the conducting plate attracts the bunch with a force increasing with the bunch displacement from the midplane. The phenomenon, involving the transverse movement of the bunch as a whole, arises from image forces and could lead to a transverse instability of the beam. This is discussed further in Sect. 6.

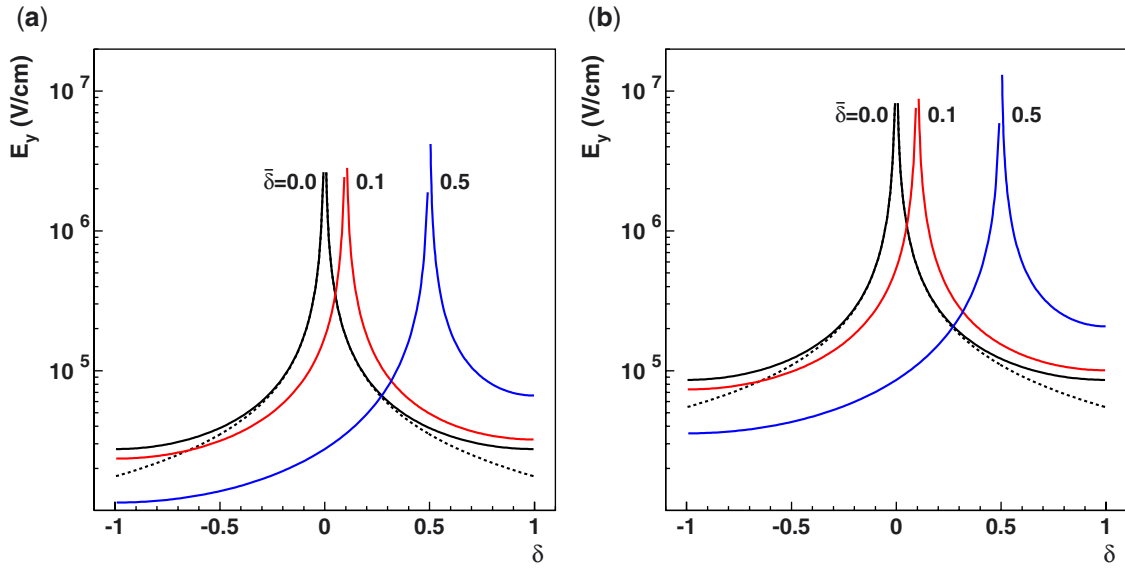


Fig. 5. The electric field strength distribution in a gap between parallel conducting plates (solid curves) and in free space (dashed curves) at several values of the bunch offset $\bar{\delta}$. (a) The LHC nominal proton beam scenario with parameters as they are given in Table 1. (b) An ILC-like positron beam, $N = 2.0 \times 10^{10}$, $a = 17 \mu\text{m}$, $\sigma_z = 300 \mu\text{m}$, and $h = 1.4 \text{ cm}$.

$\bar{\delta} = 0$, $\delta = 1$: the bunch is in the midplane and the observation point is at the plate, $y = h$:

$$\Lambda(1, 0) = \frac{1}{2} \left(\frac{\pi}{2} - 1 \right). \quad (39)$$

The image field (36) must be added to the direct field of the bunch (32) to meet the boundary condition at conducting surfaces. It is interesting to note that the last term in Eq. (37) is opposite in sign to the direct field contribution outside the bunch and cancels it. As a result, the electric field distribution between parallel conducting plates is given by

$$E_{y,\text{tot}}(y, \bar{y}, z, t) = E_{y,\text{dir}} + E_{y,\text{im}} = \kappa \frac{q\lambda(z, t)}{h} \frac{\pi \cdot \cos(\frac{\pi}{2}\bar{\delta})}{\sin(\frac{\pi}{2}\delta) - \sin(\frac{\pi}{2}\bar{\delta})}. \quad (40)$$

In particular, a bunch moving in the midplane generates the field described by

$$E_{y,\text{tot}}(y, 0, z, t) = \kappa \frac{2q\lambda(z, t)}{h} \cdot \frac{\pi/2}{\sin(\frac{\pi}{2}\delta)}. \quad (41)$$

In other words, in the presence of conducting plates the electric field in front of the plate is enhanced by the factor $\pi/2$ (Fig. 5).

If now we do not assume that the bunch offset $\bar{\delta}$ is small then the full linear approximation in δ can be derived by means of Eqs. (A.8) and (A.14) from Appendix A. Thus, the vertical component of the electric field seen by a test particle in the vicinity of the bunch ($|\delta - \bar{\delta}| \ll 1$) is given by

$$E_{y,\text{tot}}(y, \bar{y}, z, t) \approx \kappa \frac{2q\lambda(z, t)}{h} \left[\frac{1}{\delta - \bar{\delta}} + \frac{\pi}{4} \tan\left(\frac{\pi}{2}\bar{\delta}\right) + 2\epsilon_1(\bar{\delta})(\delta - \bar{\delta}) \right]. \quad (42)$$

Here we have introduced a generalization of the Laslett electric image coefficient ϵ_1 in the case of an arbitrary offset:

$$\epsilon_1(\bar{\delta}) = \frac{\pi^2}{32} \left[\frac{1}{\cos^2(\frac{\pi}{2}\bar{\delta})} - \frac{1}{3} \right], \quad \epsilon_1(0) = \frac{\pi^2}{48}. \quad (43)$$

This approximation has to be compared with an alternative representation of Eq. (40) in the form (A.8):

$$E_{y,\text{tot}}(y, \bar{y}, z, t) = \kappa \frac{2q\lambda(z, t)}{h} \frac{\pi}{4} \left\{ \tan \left[\frac{\pi}{4}(\delta + \bar{\delta}) \right] + \cot \left[\frac{\pi}{4}(\delta - \bar{\delta}) \right] \right\}, \quad (44)$$

to show the origin of each term in Eq. (42). The potential function of the field (44) is

$$U_{\text{tot}}(y, \bar{y}) = 2q\kappa\lambda \left\{ \ln \cos \left[\frac{\pi}{4}(\delta + \bar{\delta}) \right] - \ln \sin \left[\frac{\pi}{4}(\delta - \bar{\delta}) \right] \right\}, \quad (45)$$

with $E_{y,\text{tot}} = -\partial U/\partial y$.

In the linear approximation one can obtain the horizontal component of the electric image field directly from

$$\nabla \vec{E}_{\text{im}} = \frac{\partial E_{x,\text{im}}}{\partial x} + \frac{\partial E_{y,\text{im}}}{\partial y} = 0, \quad (46)$$

with the use of Eqs. (A.14) and (36). Thus,

$$E_{x,\text{im}}(x, \bar{y}, z, t) \approx -\kappa \frac{4q\lambda(z, t)}{h} \epsilon_1(\bar{\delta}_y) \delta_x, \quad (47)$$

$$E_{y,\text{im}}(y, \bar{y}, z, t) \approx \kappa \frac{4q\lambda(z, t)}{h} \left[\frac{\pi}{8} \tan\left(\frac{\pi}{2}\bar{\delta}_y\right) + \epsilon_1(\bar{\delta}_y)(\delta_y - \bar{\delta}_y) \right], \quad (48)$$

with $\delta_x = x/h$, $\delta_y = y/h$, and $\bar{\delta}_y = \bar{y}/h$. As follows from Eqs. (35) and (36), the image fields produce defocusing forces in the y -direction. On the other hand, due to Eq. (47), the corresponding forces in the x -direction produce focusing forces.

Equations (42) and (44) tell us that with an increase of $\bar{\delta}_y$, the field strength near the bunch and the field gradient across the bunch, $\partial E_{y,\text{im}}/\partial y \sim 1/\cos^2(\frac{\pi}{2}\bar{\delta}_y)$, significantly increase. This is illustrated by Fig. 5, which shows that with an increase of $\bar{\delta}_y$ the field distribution between plates becomes more and more asymmetric. At the opposite ends of the bunch diameter the difference in the value of the field, $\Delta E_{y,\text{tot}}(\bar{\delta}_y)$, grows as the displacement increases. For the LHC beam one gets $\Delta E_{y,\text{tot}}(0.1) = 4360$ V/cm, $\Delta E_{y,\text{tot}}(0.5) = 27\,290$ V/cm, and for the ILC beam $\Delta E_{y,\text{tot}}(0.1) = 13\,640$ V/cm and $\Delta E_{y,\text{tot}}(0.5) = 85\,340$ V/cm, respectively. In Sect. 6 we discuss how this effect modifies the tune shifts.

5. Magnetic images

In the above, we have discussed electric image fields created by an ultra-relativistic bunch. Magnetic images can be treated in much the same way [13,22]. Let the ferromagnetic boundaries be represented by a pair of infinitely wide parallel plates at $y = +g$ and $y = -g$. The magnetic field lines must enter

the magnet pole faces perpendicularly. For magnetic image fields we distinguish between DC and AC image fields. The DC field penetrates the metallic vacuum chamber and reaches the ferromagnetic poles. In the case of bunched beams the AC fields are of rather high frequency, and we assume that they do not penetrate the thick metallic vacuum chamber. The DC Fourier component of a bunched beam current is equal to twice the average beam current $J = qc\beta\lambda\mathcal{B}$ [13], where \mathcal{B} is the Laslett bunching factor.

A magnetic field, seen by a particle at location y on the y -axis, is generated by successive image currents with the same sign as the beam itself. In Appendix B it is proven that the resulting field is described by

$$B_{x,\text{im,DC}}(y, \bar{y}, z) = \frac{4\kappa q\beta\lambda(z)}{gc} \mathcal{B} \cdot H(\eta_y, \bar{\eta}_y). \tag{49}$$

Here we have made the replacement $\mu_0 = 1/(\epsilon_0 c^2)$ and used the scaled variables $\eta_y = y/g$ and $\bar{\eta}_y = \bar{y}/g$; $\mathcal{B} = n_b L / 2\pi R$ is the bunching factor, n_b the number of bunches, R the average accelerator radius. The structure function H is of the form

$$H(\eta_y, \bar{\eta}_y) = \frac{1}{2} \left[\frac{1}{\eta_y - \bar{\eta}_y} - \frac{\pi}{2} \cdot \frac{\cos(\frac{\pi}{2}\eta_y)}{\sin(\frac{\pi}{2}\eta_y) - \sin(\frac{\pi}{2}\bar{\eta}_y)} \right]. \tag{50}$$

In the functional sense, $H(\eta_y, \bar{\eta}_y) = \Lambda(\bar{\eta}_y, \eta_y)$, as can be noticed by comparing Eqs. (50) and (37).

In the linear approximation in y and \bar{y} one obtains from the exact formula (50) (see Appendix B for details)

$$B_{x,\text{im,DC}}(y, \bar{y}) \simeq \frac{4\kappa q\beta\lambda(z)}{g^2 c} \mathcal{B} \epsilon_2 \cdot (y + \frac{1}{2}\bar{y}), \tag{51}$$

where $\epsilon_2 = \pi^2/24$ is the Laslett form factor for infinite parallel plate magnet poles⁴. As above for electric images, we define a generalized form of ϵ_2 for an arbitrary offset $\bar{\eta}_y$ as follows:

$$\epsilon_2(\bar{\eta}_y) = \frac{\pi^2}{32} \left[\frac{1}{\cos^2(\frac{\pi}{2}\bar{\eta}_y)} + \frac{1}{3} \right], \quad \epsilon_2(0) = \frac{\pi^2}{24}. \tag{52}$$

Thus, the complete linear approximations in η_x and η_y (see Appendix B) are given by

$$B_{x,\text{im,DC}}(y, \bar{y}, z) \simeq \frac{4\kappa q\beta\lambda(z)}{gc} \mathcal{B} \left[\frac{\pi}{8} \tan(\frac{\pi}{2}\bar{\eta}_y) + \epsilon_2(\bar{\eta}_y)(\eta_y - \bar{\eta}_y) \right] \tag{53}$$

and

$$B_{y,\text{im,DC}}(x, \bar{y}, z) \simeq \frac{4\kappa q\beta\lambda(z)}{gc} \mathcal{B} \epsilon_2(\bar{\eta}_y) \eta_x. \tag{54}$$

For further applications, we point out that on the bunch axis, $\eta_y = \bar{\eta}_y$, from Eq. (B.5) one gets

$$H(\bar{\eta}_y, \bar{\eta}_y) = \frac{\pi}{8} \tan(\frac{\pi}{2}\bar{\eta}_y). \tag{55}$$

⁴ In Ref. [13] Eq. (18.57) should be read with the factor $(y + \bar{y}/2)$ as in Eq. (51).

The contribution of the magnetic AC image field due to eddy currents in vacuum chamber walls is similar to electric image fields,

$$B_{x,\text{im,AC}}(y, \bar{y}, z) = -\frac{4\kappa q\beta\lambda(z)}{hc}(1 - \mathcal{B}) \cdot \Lambda(\delta_y, \bar{\delta}_y), \quad (56)$$

and therefore

$$B_{y,\text{im,AC}}(x, \bar{y}, z) = -\frac{4\kappa q\beta\lambda(z)}{hc}(1 - \mathcal{B})\epsilon_1(\bar{\delta}_y)\delta_x, \quad (57)$$

where the factor $(1 - \mathcal{B})$ accounts for the subtraction of the DC component. Thus, at $\delta_x = 0$ the net AC field is tangential to the surface.

The magnetic image fields must be added to the direct magnetic field (2) to meet the boundary condition at ferromagnetic surfaces. That is, the summary horizontal component of the magnetic field between the conducting plates is

$$\begin{aligned} B_{x,\text{tot}}(y, \bar{y}) &= B_{x,\text{dir}} + B_{x,\text{im,DC}} + B_{x,\text{im,AC}} \\ &= -\frac{\pi\kappa q\beta\lambda}{hc} \left\{ \frac{(1 - \mathcal{B}) \cos[(\pi/2)\bar{\delta}_y]\theta(1 - \delta_y)}{\sin[(\pi/2)\delta_y] - \sin[(\pi/2)\bar{\delta}_y]} + \frac{h}{g} \cdot \frac{\mathcal{B} \cos[(\pi/2)\eta_y]}{\sin[(\pi/2)\eta_y] - \sin[(\pi/2)\bar{\eta}_y]} \right\}. \end{aligned} \quad (58)$$

The step function $\theta(1 - \delta_y)$ accounts for the fact that the AC fields do not penetrate the thick metallic vacuum chamber. For a more detailed discussion of the subject see Refs. [23,24].

6. Image forces and tune shifts

Direct space-charge fields, as well as fields due to image charges and currents, shift the betatron frequencies (tunes). We have to distinguish between coherent tune shifts, which express a change of the betatron frequency when the bunch oscillates as a whole, and incoherent tune shifts, which change the single particle tune. In this section we again assume the bunch to have a circular cross section of radius a and a uniform density.

In the next two subsections we restrict our analysis to an idealized case of a vacuum chamber and/or ferromagnetic poles as two infinite parallel plates and the motion of a bunch in the vertical y -direction⁵. Infinite parallel plates are a good approximation for finite-width collimator parallel plates, given the small transverse beam size in modern accelerators. Our equations for tune shifts are valid at an arbitrary bunch offset and presented in notations as given in Refs. [14] and [25]. This allows us to compare results obtained by different authors. In Sect. 6.3 we consider a more realistic example of a finite-length collimator with parallel conducting jaws.

6.1. Coherent motion and tune shift

The motion of the bunch center $\bar{\delta}(s)$ in the absence of an external focusing force is described by the equation

$$\frac{d^2\bar{\delta}(s)}{ds^2} = \frac{F_{y,\text{im}}}{M_b\gamma h\beta^2 c^2}, \quad (59)$$

⁵ For this reason, below we omit the subscripts x and y for variables δ and η . If there are no ferromagnetic poles, one has to set $g = \infty$ in each equation below.

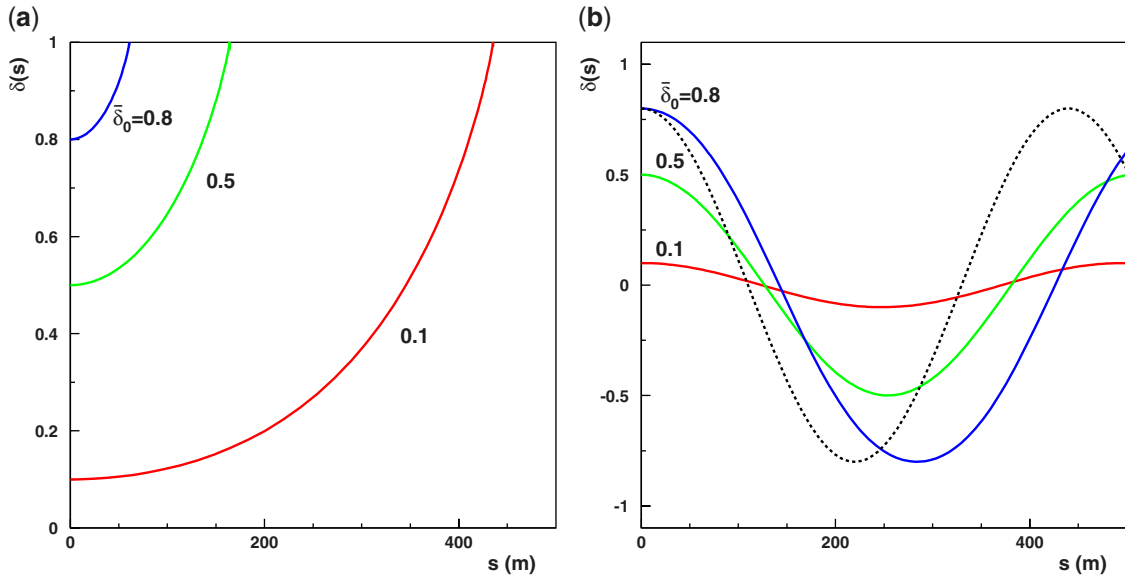


Fig. 6. Numerical solutions of Eqs. (59) and (62). The dependence of the bunch trajectory along the beam path on the initial value $\bar{\delta}_0$. (a) The linear focusing is switched off, transverse motion only under the influence of the image forces. The bunch impacts the plate at $\delta(s_i) = 1$. (b) The coherent oscillation of the bunch under the influence of the linear focusing and image forces (solid lines). The dashed line shows the betatron oscillation at $\bar{\delta}_0 = 0.8$ without taking account of the image forces, $\mathcal{I} = 0$.

where $s = \beta ct$ and the Lorentz force is of the form

$$\begin{aligned}
 F_{y,\text{im}} &= Q_b(E_{y,\text{im}} + \beta c B_{x,\text{im}}) \\
 &= \frac{4\kappa Q_b q \lambda}{h} \left[\left(\frac{1}{\gamma^2} + \beta^2 \mathcal{B} \right) \Lambda(\delta, \bar{\delta}) + \beta^2 (h/g) \mathcal{B} H(\eta, \bar{\eta}) \right].
 \end{aligned}
 \tag{60}$$

Here we have applied the results of the previous section; $M_b = Nm_p$ is the bunch mass, $Q_b = Nq$ the bunch charge. On the bunch axis, the electric and magnetic structure functions are

$$\Lambda(\bar{\delta}, \bar{\delta}) = \frac{\pi}{8} \tan\left(\frac{\pi}{2} \bar{\delta}\right), \quad H(\bar{\eta}, \bar{\eta}) = \frac{\pi}{8} \tan\left(\frac{\pi}{2} \bar{\eta}\right).
 \tag{61}$$

Under the influence of the force (60) the bunch is attracted by a conducting plate and at some point s_i hits the plate. The actual position of the impact point depends on the initial value constraints, in particular, the bunch offset $\bar{\delta}(0) = \bar{\delta}_0$. Figure 6(a) shows the numerical solutions of Eq. (59) with a set of initial conditions $(\bar{\delta}_0, \bar{\delta}'_0 = 0)$ at $\bar{\delta}_0 = 0.1, 0.5, 0.8$. For example, let protons in the bunch be at the energy 7 TeV and the machine parameters are as in Table 1 [26]. Then the impact points $s_i(\bar{\delta}_0)$ are located at distances $s_i(0.1) = 453.3$ m, $s_i(0.5) = 164.2$ m, and $s_i(0.8) = 61.0$ m, respectively.

It should be noted that Eq. (59) is true in the approximation, when the bunch velocity along the z -axis is constant, and much larger than the drift velocity in the y direction, $v_z \simeq \beta c \gg v_y$. In this case, the bunch path is a smooth curve, as shown in Fig. 6(a). However, with a more rigorous account of the effect of crossed electric and magnetic fields from the images, it is necessary to solve together a system of two coupled differential equations for movements along the z and y directions. In this case, the bunch trajectory is a cycloid-like curve.

The coherent motion of the bunch in the y -direction is significantly altered in the presence of the linear focusing provided by quadrupoles and described by the equation

$$\frac{d^2\bar{\delta}(s)}{ds^2} + K_0^2\bar{\delta}(s) - \mathcal{I}\left\{\frac{\pi}{2}\left(\frac{1}{\mathcal{B}\beta^2\gamma^2} + 1\right)\tan\left[\frac{\pi}{2}\bar{\delta}(s)\right] + \frac{\pi h}{2g}\tan\left[\frac{\pi h}{2g}\bar{\delta}(s)\right]\right\} = 0. \quad (62)$$

Here

$$K_0^2 = \left(\frac{v_0}{R}\right)^2, \quad \mathcal{I} = \frac{r_p\lambda\mathcal{B}}{h^2\gamma},$$

where $r_p = \kappa q^2/m_p c^2$ is the classical proton radius and the meaning of the other parameters is explained in Table 1. With the values of the parameters⁶ from Table 1, $K_0^2 = 2.041 \times 10^{-4} \text{ m}^{-2}$ and $\mathcal{I} = 1.73 \times 10^{-5} \text{ m}^{-2}$. Thus, for small $\bar{\delta}_0$ the linear focusing is a driving force.

Figure 6(b) shows numerical solutions of Eq. (62) for the same initial conditions as above. The dashed line shows a solution of the betatron equation (62) in the absence of the image effects, $\mathcal{I} = 0$. A comparison of the two curves at $\bar{\delta}_0 = 0.8$ demonstrates how big the influence of images on the coherent tune shift is.

To derive an analytical expression for the coherent tune shift for an arbitrary offset we proceed in the standard way [14,22,23]. In the linear theory, we assume that the forces are proportional to the displacement. Therefore, we expand the structure functions Λ and H (61) in a power series in the neighborhood of $\bar{\delta}_0$, $\bar{\delta} = \bar{\delta}_0 + \Delta$, keeping only terms up to first order in Δ :

$$\Lambda(\bar{\delta}_0, \Delta) = \frac{\pi}{8}\tan\left[\frac{\pi}{2}(\bar{\delta}_0 + \Delta)\right] \approx \frac{\pi}{8}\tan\left(\frac{\pi}{2}\bar{\delta}_0\right) + \xi_1(\bar{\delta}_0)\Delta(s), \quad (63)$$

$$H(\bar{\eta}_0, \Delta) \approx \frac{\pi}{8}\tan\left(\frac{\pi}{2}\bar{\eta}_0\right) + \frac{h}{g}\xi_2(\bar{\eta}_0)\Delta(s). \quad (64)$$

Here we have introduced generalized Laslett coherent tune shift form factors,

$$\begin{aligned} \xi_1(\bar{\delta}) &= \frac{\pi^2}{16\cos^2(\frac{\pi}{2}\bar{\delta})}, & \xi_1(0) &= \frac{\pi^2}{16}, \\ \xi_2(\bar{\eta}) &= \frac{\pi^2}{16\cos^2(\frac{\pi}{2}\bar{\eta})}, & \xi_2(0) &= \frac{\pi^2}{16}, \end{aligned} \quad (65)$$

for the image fields from the vacuum chamber and the magnet pole. Substituting expressions for $\Lambda(\bar{\delta}_0, \Delta)$ and $H(\bar{\eta}_0, \Delta)$ in Eq. (62), we get⁷

$$\Delta v_y^{(\text{coh})}(\bar{\delta}_0) = -\frac{R\langle\hat{\beta}\rangle}{2m_p c^2 \gamma \beta^2} \frac{\partial F_{y,\text{im}}}{\partial y} = -\frac{2r_p J R \langle\hat{\beta}\rangle}{q\beta c \gamma} \left[\left(\frac{1}{\mathcal{B}\beta^2\gamma^2} + 1\right) \frac{\xi_1(\bar{\delta}_0)}{h^2} + \frac{\xi_2(\bar{\eta}_0)}{g^2} \right]. \quad (66)$$

One must note that the image coefficients ϵ_1 and ξ_1 , as well as ϵ_2 and ξ_2 , are not independent but are rooted in the same function $\Lambda(\delta, \bar{\delta})$ and $H(\eta, \bar{\eta})$, correspondingly. Therefore, in the linear approximation these functions are related via

$$\epsilon_1(\bar{\delta}) = \frac{1}{2}\left[\xi_1(\bar{\delta}) - \frac{\pi^2}{48}\right], \quad \epsilon_2(\bar{\eta}) = \frac{1}{2}\left[\xi_2(\bar{\eta}) + \frac{\pi^2}{48}\right]. \quad (67)$$

⁶ With $v_{y0} \simeq v_{x0} = v_0$.

⁷ We add a hat to the amplitude function $\hat{\beta}$ to avoid confusion with the relativistic velocity β .

Table 1. The LHC machine and beam parameters [26] used in calculation of the coherent and incoherent tune shifts.

h , collimator half-gap	[m]	1.2×10^{-3}
g , magnet poles half-gap	[m]	4.0×10^{-2}
N , bunch population		1.15×10^{11}
σ_z , r.m.s. bunch length	[m]	7.55×10^{-2}
a , r.m.s. bunch radius	[m]	1.67×10^{-5}
\mathcal{B} , bunching factor		0.1993
$\lambda = N/\sqrt{2\pi}\sigma_z$, linear density		
$J = q\beta c\lambda\mathcal{B}$, average beam current		
m_p , proton mass	[GeV]	0.938
γ , Lorentz factor		7463
$\nu_0 = R/\langle\hat{\beta}\rangle$, betatron tune		60.61
$\langle\hat{\beta}\rangle$, average $\hat{\beta}$ -function	[m]	70
$2\pi R$, ring circumference	[m]	26 658.883

6.2. Incoherent tune shifts

Let us now evaluate the effect of the image forces on the betatron oscillation of the particles in a bunch. The motion of a test particle in a displaced bunch in the presence of the space-charge force and the image fields is described by the equation

$$\frac{d^2\delta}{ds^2} + K_0^2\delta = \frac{(F_{y,sc} + F_{y,im})}{mh\gamma\beta^2c^2}. \quad (68)$$

Here $F_{y,sc} = 2\kappa q^2\lambda y/a^2\gamma^2$ is the Lorentz force due to the bunch space-charge [13] and $F_{y,im}$ is defined in Eq. (60). Inserting the linear approximations (A.14) and (B.7) into Eq. (68), in the same manner as above one gets a vertical tune shift:

$$\Delta\nu_y^{(inc)}(\bar{\delta}) = -\frac{2r_pJR\langle\beta\rangle}{q\beta c\gamma} \left[\frac{1}{\mathcal{B}\beta^2\gamma^2} \left(\frac{1}{2a^2} + \frac{\epsilon_1(\bar{\delta})}{h^2} \right) + \frac{\epsilon_1(\bar{\delta})}{h^2} + \frac{\epsilon_2(\bar{\delta})}{g^2} \right]. \quad (69)$$

The above analysis can be carried out similarly for the x -motion. The result is

$$\Delta\nu_x^{(inc)}(\bar{\delta}) = \frac{2r_pJR\langle\beta\rangle}{q\beta c\gamma} \left[\frac{1}{\mathcal{B}\beta^2\gamma^2} \left(\frac{\epsilon_1(\bar{\delta})}{h^2} - \frac{1}{2a^2} \right) + \frac{\epsilon_1(\bar{\delta})}{h^2} + \frac{\epsilon_2(\bar{\delta})}{g^2} \right]. \quad (70)$$

Equations (66), (69), and (70) generalize the Laslett tune shifts to the case of the arbitrary bunch offset between parallel conducting plates and ferromagnetic poles.

As numerical examples, with machine and beam parameters from Table 1, let us compare the contribution of each term in Eq. (69) at two distinct values of $\bar{\delta}$, $\bar{\delta} = 0$ and $\bar{\delta} = 0.8$:

$$\begin{aligned} \Delta\nu_y^{(inc)}(0) &= -(3.8 \times 10^{-4} + 1.9 \times 10^{-7} + 2.113 + 3.8 \times 10^{-3}) \approx -2.117, \\ \Delta\nu_y^{(inc)}(0.8) &= -(3.8 \times 10^{-4} + 2.9 \times 10^{-6} + 32.136 + 3.81 \times 10^{-3}) \approx -32.14. \end{aligned}$$

Thus, the third term gives the main contribution that increases with $\bar{\delta}$, and the transverse particle dynamics in a bunch is defined by the influence of electric images.

6.3. Collimator of a finite length

The representation of a vacuum chamber and magnetic poles in the form of infinite parallel plates is a very useful mathematical abstraction. However, in real accelerators, all components are finite in

size and at the same time some of these components include elements that are structurally designed as parallel conductive and ferromagnetic flat surfaces. In circular accelerators such as LHC [26] and the future HL-LHC [27], flat parallel surfaces are parts of different types of collimators, the normal conducting separator and orbit correction dipole magnets⁸. As a rule, collimator jaws have a length of 600–1400 mm, and their width is about 50 mm. Similarly, the poles of a dipole magnet have a length of 2000–3400 mm and a pole width of 60 mm [27]. With transverse beam sizes as small as 200 μm , the representation of collimators and dipole magnets in the form of infinite parallel plates is a good approximation for these elements and it is legitimate to apply here the results obtained in the previous sections.

Suppose that the accelerator ring only includes one collimator at point s_0 . A collimator is a short straight section of an accelerator and does not have a guide magnetic field. The motion of the bunch center $\bar{\delta}$ in the collimator is therefore described by Eq. (59), with $F_{y,\text{im}}$ from Eq. (60), where we set $g = \infty$. In the rest of a circular accelerator the motion of the bunch is described by Eq. (62) with $\mathcal{I} = 0$.

Now we would like to derive in the framework of linear theory an analytical expression for the coherent tune shift due to the image effects in a finite-size collimator. For more than a single collimator one would simply add the individual contribution from each collimator to find the total tune shift.

The image fields $E_{y,\text{im}}$ and $B_{x,\text{im,AC}}$ act along the same line, so we introduce the effective field B_{eff} and decompose it into dipole-like and quadrupole-like parts with the use of Eqs. (36), (56), and (63),

$$B_{\text{eff}} = B_{x,\text{im,AC}} + E_{y,\text{im}}/\beta c = B_D + G_{\text{eff}} \cdot \Delta(s), \quad (71)$$

where

$$B_D = \kappa \frac{\pi q \lambda \beta \mathcal{B}}{2hc} \left(1 + \frac{1}{\mathcal{B} \beta^2 \gamma^2}\right) \tan\left(\frac{\pi}{2} \bar{\delta}_0\right), \quad G_{\text{eff}} = \kappa \frac{4q \lambda \beta \mathcal{B}}{hc} \left(1 + \frac{1}{\mathcal{B} \beta^2 \gamma^2}\right) \xi_1(\bar{\delta}_0). \quad (72)$$

Image fields act as a perturbation on the betatron oscillation of the bunch. Thus, the equation of motion of the perturbation $\Delta(s)$ of the transverse coordinate of the bunch with the offset $\bar{\delta} = \bar{\delta}_0 + \Delta$ takes the form

$$\Delta'' - K_Q \Delta(s) = K_D, \quad (73)$$

with

$$K_D = \frac{\pi}{2} \mathcal{I} \left(1 + \frac{1}{\mathcal{B} \beta^2 \gamma^2}\right) \tan\left(\frac{\pi}{2} \bar{\delta}_0\right), \quad K_Q = 4\mathcal{I} \left(1 + \frac{1}{\mathcal{B} \beta^2 \gamma^2}\right) \xi_1(\bar{\delta}_0). \quad (74)$$

As the analysis in Ref. [13], Sect. 12.1.1 shows, dipole terms of the type K_D cause a shift in the beam path without affecting the focusing properties of the beam line. In contrast, terms that depend linearly on the transverse bunch offset from the orbit will affect focusing and the stability of the transverse motion of the beam, because these perturbations act like quadrupoles.

The longitudinal size of the collimator l_c is small in comparison with the wavelength of betatron oscillations, so we consider the collimator as a point source of perturbation. Let us assume that such

⁸ A list of collimators for the LHC Run 2 (in 2015) includes 108 items and is shown on p. 151 of the technical design report “High-Luminosity Large Hadron Collider (HL-LHC)” [27].

a perturbation at point $(s_0, \bar{\delta}_0)$ is created by a thin lens of the focusing strength $\sigma_{\text{im}} = g * l_c$ [13,28]. Here $g = qG_{\text{eff}}/hm_p c \beta \gamma$, with G_{eff} from Eq. (72).

The evolution of a bunch through elements of an accelerator is most clearly described by the product of transfer matrices [13,28,29]. The transfer matrix for a full revolution is $\mathbf{M} = \mathbf{M}_p \mathbf{M}_0$, where for the lens

$$\mathbf{M}_p = \begin{pmatrix} 1 & 0 \\ \sigma_{\text{im}} & 1 \end{pmatrix} \quad (75)$$

and for the unperturbed part of the ring

$$\mathbf{M}_0 = \begin{pmatrix} \cos(\psi_0) & \hat{\beta}_0 \sin(\psi_0) \\ -\frac{1}{\hat{\beta}_0} \sin(\psi_0) & \cos(\psi_0) \end{pmatrix}. \quad (76)$$

Here $\psi_0 = 2\pi \nu_0$ is the unperturbed phase advance per turn and $\hat{\beta}_0$ is the unperturbed betatron function at the location of the perturbation, $s = s_0$. On the other hand, the perturbed transfer matrix \mathbf{M} can also be written in the form (76) if we replace $\hat{\beta}_0$ by $\hat{\beta}$ and ν_0 by ν , where ν is the the betatron tune in the presence of the field gradient, G_{eff} , from images.

By equating the traces of the perturbed matrix and the transfer matrix for a full revolution, $\text{Tr}(\mathbf{M}) = \text{Tr}(\mathbf{M}_p \mathbf{M}_0)$, with setting $\nu = \nu_0 + \Delta\nu$ and $|\Delta\nu| \ll \nu_0/2\pi$, we get the tune shift due to this perturbation:

$$\Delta\nu^{(\text{im})}(\bar{\delta}_0, h, l_c, \hat{\beta}_0) = -\frac{\hat{\beta}_0 \sigma_{\text{im}}}{4\pi} = -\frac{\hat{\beta}_0}{\pi} \mathcal{I} \left(1 + \frac{1}{\mathcal{B} \beta^2 \gamma^2} \right) \xi_1(\bar{\delta}_0) \cdot l_c. \quad (77)$$

The total tune shift is the sum of the individual contribution from each collimator:

$$\Delta\nu_{\text{tot}}^{(\text{im})} = \sum_{i=1}^{n_c} \Delta\nu^{(\text{im})}(\bar{\delta}_{0i}, h_i, l_{ci}, \hat{\beta}_{0i}), \quad (78)$$

where n_c is the number of collimators along the accelerator circumference.

As stated in Ref. [26], p. 100, the $\hat{\beta}$ -functions at the collimators range from 27–360 m and the range of collimator half-gaps h is 4.7–11.1 mm for the injection optics and 1.2–3.8 mm for the squeezed optics. On evaluating with Eq. (77) the numerical values of $\Delta\nu_c(\bar{\delta}_0)$, we set these values of $\hat{\beta}_0$, $h = 1.2$ mm, $l_c = 1$ m, and the machine and beam parameters from Table 1. The results are presented in Fig. 7.

Figure 7 shows that at $\bar{\delta}_0 < 0.6$ the total tune shift due to the quadrupole-type image fields in collimators, $\sim n_c \cdot |\Delta\nu^{\text{im}}(\bar{\delta}_0)|$, $n_c \sim 100$, does not exceed the safe value of the order of 0.1. However, if the beam offset accidentally exceeds $\bar{\delta}_0 \approx 0.6 \div 0.7$, it is possible to develop transverse instability and shift the betatron frequency into the resonance region.

7. Summary

This paper presents new analytical expressions for electric and magnetic self-fields produced by a bunch shaped as a cylinder with a circular and an elliptical cross section. Calculations are done in the relativistic limit. These expressions show the correct Coulomb asymptotic and in the near-field zone coincide with the external self-fields of a continuous beam. In the ultra-relativistic limit, external fields of a bunch takes the universal form (32) and (20).

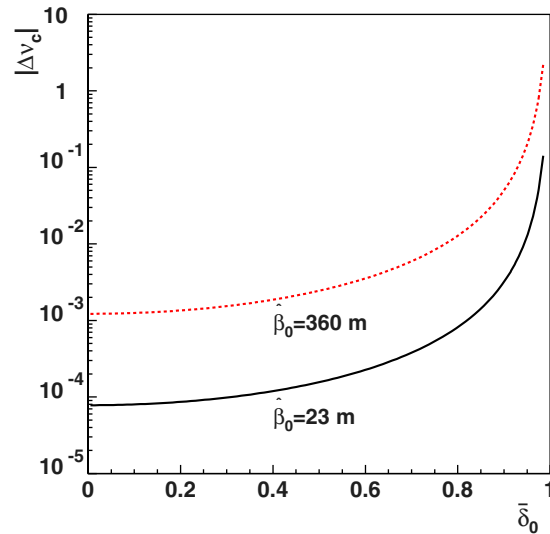


Fig. 7. Variation of $|\Delta\nu_c(\bar{\delta}_0)|$ with the bunch offset at $\hat{\beta}_0 = 23$ m and $\hat{\beta}_0 = 360$ m.

We reanalyzed the problem summation of image fields generated by a charged bunch between infinitely wide parallel conducting plates and/or ferromagnetic poles. The exact 1D solutions for resulting electric and magnetic image fields are represented by the structure functions $\Lambda(\delta, \bar{\delta})$ and $H(\eta, \bar{\eta})$, respectively.

The new expressions for modified fields are applied to study the coherent and incoherent tune shifts for both infinite and finite parallel flat surfaces and allow within an improved linear approximation generalization of the Laslett image coefficients in the case of an arbitrary bunch offset $\bar{\delta}$. These image coefficient functions, $\epsilon_1(\bar{\delta})$ and $\xi_1(\bar{\delta})$, as well as $\epsilon_2(\bar{\eta})$ and $\xi_2(\bar{\eta})$, are not now independent but are rooted in the functions $\Lambda(\delta, \bar{\delta})$ and $H(\eta, \bar{\eta})$, correspondingly. Equation (77) and Fig. 7 allow us to evaluate how the gradient of image fields in a finite-size collimator affects the betatron frequency of the beam. In particular, if the beam offset in collimators accidentally exceeds $\bar{\delta}_0 \approx 0.6 \div 0.7$, it is possible to develop transverse instability and shift the betatron frequency into the resonance region.

After a first version of the present paper became public [30] the author learned⁹ about the old textbook [31] and article [32], where only the scalar potential function of the electric field generated by a line charge between parallel earthed conducting planes is calculated with the use of conformal mapping. In addition, in Ref. [32] are calculated incoherent and coherent image coefficients. The results of Ref. [32] for the image coefficients and tune shifts were rederived in Ref. [33] and several misprints are corrected. This allows us to directly compare the results obtained by different methods.

Let us set, in Eq. (3) from Sect. 4.20 of Ref. [31], $a = 2h$, $b = h + \bar{y}$, and $x = 0$ (transition to a 1D problem). Then, by expressing hyperbolic sinh via trigonometric functions sin and cos, one exactly recovers Eq. (45). Similarly, if one sets, in Eq. (27) of Ref. [32], $x = x_1 = 0$ and $y_1 = \bar{y}$ and applies the double angle formula for cos, one gets Eq. (45). The field coefficients (29), (30), and (32) of Ref. [32] match Eqs. (43), (65), and (52) of the present paper. However, expressions for the resulting electric and magnetic fields between the conducting plates (40), (44), (58) and the relations of type (67) between image coefficients and their origin were not revealed in Ref. [32].

⁹ Special thanks to the anonymous reader for providing Refs. [31,32] and useful comments.

The two parallel infinite plates is a particular case of a rectangular vacuum chamber when the width to height w/h of the rectangle goes to infinity. In Ref. [33] this limit was considered only for a centered beam, $\bar{\delta} = 0$. The electric and magnetic image coefficients as well as the tune shift coefficients are of the same values as $\epsilon_{1,2}(0)$ and $\xi_{1,2}(0)$ above. The equations for the vertical and horizontal, incoherent and coherent betatron tune shifts [33], after some rearrangements and neglecting the neutralization factor, take the same form as Eqs. (66), (69), and (70) at $\bar{\delta} = \bar{\eta} = 0$.

Tune shifts and Laslett coefficients for a rectangular and a circular beam pipe were also calculated in Refs. [24,34]. Due to the fact that the radial and vertical betatron oscillations are coupled in general, the tune shift and image coefficients accordingly form second-rank tensors. We can state a guess that the relations of type (67) are somehow connected with this fact; see Eq. (15) in Ref. [34]. However, in Ref. [34] explicit formulas have been given only for a square vacuum chamber, $w = h$; therefore the passage to the limit of parallel plates is impossible.

To conclude, the results presented here can serve as a starting point in applying the method of images to find exact solutions in 2D problems, calculating the field emission current in a collimator and a study of beam-induced multipacting. All these problems are relevant for the High-Luminosity Large Hadron Collider under construction [35].

Acknowledgements

The author is grateful to P. Bussey, E. Lohrmann, M. Dohlus, and F. Willeke for reading the early version of the manuscript, comments, and useful discussions. I would like to express my special gratitude to E. Osborneva for her support and discussion of the results.

Appendix A. Electric image fields

Here we derive the formula (37).

Let us split the contribution of all image fields (34) given in braces into two parts,

$$\begin{aligned} & (2h - y_1)^{-1} - (2h + y_1)^{-1} - (4h - y_2)^{-1} + (4h + y_2)^{-1} \\ & + (6h - y_1)^{-1} - (6h + y_1)^{-1} - (8h - y_2)^{-1} + (8h + y_2)^{-1} \\ & + (10h - y_1)^{-1} - (10h + y_1)^{-1} - (12h - y_2)^{-1} + (12h + y_2)^{-1} + \dots \end{aligned} \tag{A.1}$$

$$= \sum_k^{\infty} \Pi_k^{(-)}(y_1, h) - \sum_m^{\infty} \Pi_m^{(+)}(y_2, h), \tag{A.2}$$

where $\Pi_k^{(-)}$ represents the contribution from the negatively charged images and $\Pi_m^{(+)}$ is the contribution from the positively charged images:

$$\Pi_k^{(-)}(y_1, h) = \frac{1}{2kh - y_1} - \frac{1}{2kh + y_1} = \frac{2}{h} \cdot \frac{\delta_1}{(2k)^2 - \delta_1^2}, \tag{A.3}$$

$$\Pi_m^{(+)}(y_2, h) = \frac{1}{2mh - y_2} - \frac{1}{2mh + y_2} = \frac{2}{h} \cdot \frac{\delta_2}{(2m)^2 - \delta_2^2}. \tag{A.4}$$

Here and hereinafter, indexes k and m have odd, $k = 1, 3, 5, \dots$, and even, $m = 2, 4, 6, \dots$, values, $\delta_1 = y_1/h$ and $\delta_2 = y_2/h$.

Now it is evident that the space structure of the image fields between plates is described by a specific function $\Lambda(\delta_1, \delta_2)$; we term this the structure function:

$$\sum_k^\infty \Pi_k^{(-)} - \sum_m^\infty \Pi_m^{(+)} = \frac{2}{h} \Lambda(\delta_1, \delta_2), \tag{A.5}$$

with

$$\Lambda(\delta_1, \delta_2) = \delta_1 \sum_k^\infty \frac{1}{(2k)^2 - \delta_1^2} - \delta_2 \sum_m^\infty \frac{1}{(2m)^2 - \delta_2^2}. \tag{A.6}$$

The structure function Λ depends only on the scaled variables.

To proceed further, recall the decompositions (1.421) [36]

$$\begin{aligned} \tan\left(\frac{\pi}{2}z\right) &= \frac{4}{\pi}z \sum_{n=1}^\infty \frac{1}{(2n-1)^2 - z^2}, \\ \cot(\pi z) &= \frac{1}{\pi z} - \frac{2z}{\pi} \sum_{n=1}^\infty \frac{1}{n^2 - z^2}. \end{aligned} \tag{A.7}$$

After some algebraic manipulation and the use of Eq. (A.7), we get from Eq. (A.6) a new exact and compact expression of the structure function:

$$\Lambda(\delta_1, \delta_2) = \frac{1}{2} \left[\frac{\pi}{4} \tan\left(\frac{\pi}{4}\delta_1\right) + \frac{\pi}{4} \cot\left(\frac{\pi}{4}\delta_2\right) - \frac{1}{\delta_2} \right]. \tag{A.8}$$

Now, if we recall that $\delta_1 = (y + \bar{y})/h = \delta + \bar{\delta}$ and $\delta_2 = (y - \bar{y})/h = \delta - \bar{\delta}$, we obtain

$$\Lambda(\delta, \bar{\delta}) = \frac{1}{2} \left[\frac{\pi}{2} \cdot \frac{\cos(\frac{\pi}{2}\bar{\delta})}{\sin(\frac{\pi}{2}\delta) - \sin(\frac{\pi}{2}\bar{\delta})} - \frac{1}{\delta - \bar{\delta}} \right]. \tag{A.9}$$

For some applications it is more practical to use the relations between the Bernoulli numbers and the trigonometric functions. To do this, recall the decompositions (1.411) [36]

$$\begin{aligned} z \cdot \tan(z) &= \sum_{n=1}^\infty \frac{(2^{2n} - 1)(2z)^{2n}}{(2n)!} |B_{2n}|, \\ z \cdot \cot(z) &= 1 - \sum_{n=1}^\infty \frac{(2z)^{2n}}{(2n)!} |B_{2n}|, \end{aligned} \tag{A.10}$$

where B_{2n} are Bernoulli numbers, $B_2 = 1/6$, $B_4 = -1/30$, $B_6 = 1/42$ etc. After substituting Eq. (A.10) in Eq. (A.8), we find the following form of the structure function:

$$\Lambda(\delta_1, \delta_2) = \frac{1}{2} \sum_{n=1}^\infty \left[(2^{2n} - 1) \delta_1^{2n-1} - \delta_2^{2n-1} \right] \frac{\pi^{2n}}{2^{2n}(2n)!} |B_{2n}|. \tag{A.11}$$

Using only the linear terms, we recover the part derived by Laslett [7] (see Eq. (35)):

$$\Lambda(\delta, \bar{\delta}) = \frac{1}{h} \cdot \epsilon_1(y + 2\bar{y}). \tag{A.12}$$

An inspection of Eq. (A.11) shows that the contributions of negatively charged images are enhanced by the factor $2^{2n} - 1$, as compared with the contributions from the positively charged images. Equation (A.11) also shows that for y on the bunch axis, i.e., $\delta_2 = 0$, the contributions from the positively charged images vanish.

At first glance, Eqs. (A.8) or (A.9) are singular at $\delta_2 = 0$ or $\delta = \bar{\delta}$, respectively. However, this is not the case. Starting once again from Eq. (A.11) with $\delta_2 = 0$ and taking Eq. (A.10) into account, we formally get

$$\Lambda(\bar{\delta}, \bar{\delta}) = \frac{\pi}{8} \tan\left(\frac{\pi}{2}\bar{\delta}\right). \tag{A.13}$$

Knowing the exact form of $\Lambda(\delta, \bar{\delta})$, one is able to develop a variety of approximation. For instance, to study particle dynamics in a bunch with a significant offset, one needs to decompose Eq. (A.8) assuming $\delta_2 \ll 1$. The result is

$$\Lambda(\bar{\delta}, \delta_2) \simeq \Lambda(\delta_1, \delta_2)|_{\delta_2=0} + \left. \frac{\partial \Lambda}{\partial \delta_2} \right|_{\delta_2=0} \cdot \delta_2 = \frac{\pi}{8} \tan\left(\frac{\pi}{2}\bar{\delta}\right) + \frac{\pi^2}{32} \left[\frac{1}{\cos^2(\frac{\pi}{2}\bar{\delta})} - \frac{1}{3} \right] \delta_2. \tag{A.14}$$

Appendix B. Magnetic image fields

Let the boundary of magnet pole faces be represented as two parallel plates located at $y = \pm g$. A magnetic field, seen by a particle at location y on the y -axis, is generated by the successive image currents with the same sign as the beam itself [14,22]. Therefore, instead of the series (A.1) we get

$$\begin{aligned} & (2g - y_1)^{-1} - (2g + y_1)^{-1} + (4g - y_2)^{-1} - (4g + y_2)^{-1} \\ & + (6g - y_1)^{-1} - (6g + y_1)^{-1} + (8g - y_2)^{-1} - (8g + y_2)^{-1} \\ & + (10g - y_1)^{-1} - (10g + y_1)^{-1} + (12g - y_2)^{-1} - (12g + y_2)^{-1} + \dots \end{aligned} \tag{B.1}$$

$$\begin{aligned} & = \sum_k \Pi_k(y_1, g) + \sum_m \Pi_m(y_2, g) \\ & = \frac{2}{g} H(\eta_1, \eta_2) \end{aligned} \tag{B.2}$$

where Π_k and Π_m are of the same functional form as Eqs. (A.3) and (A.4) with an interchange of variables $h \rightarrow g$, $\delta_1 \rightarrow \eta_1 = y_1/g$, $\delta_2 \rightarrow \eta_2 = y_2/g$. Indexes k and m have odd, $k = 1, 3, 5, \dots$, and even, $m = 2, 4, 6, \dots$, values, respectively.

Now, if we are to proceed in the same manner as in Appendix A, we obtain from Eq. (B.2) an expression for the structure function of the image magnetic fields:

$$H(\eta_1, \eta_2) = \frac{1}{2} \sum_{n=1}^{\infty} \left[(2^{2n} - 1) \eta_1^{2n-1} + \eta_2^{2n-1} \right] \frac{\pi^{2n}}{2^{2n} (2n)!} |B_{2n}|. \tag{B.3}$$

For $|y| \ll g$ and $|\bar{y}| \ll g$, this gives, to first order in η_1 and η_2 ,

$$H(y, \bar{y}) = \frac{\epsilon_2}{g} \cdot (y + \frac{1}{2}\bar{y}) = \epsilon_2 (\eta + \frac{1}{2}\bar{\eta}). \tag{B.4}$$

The use of Eq. (A.10) in Eq. (B.3) gives the magnetic structure function that we are looking for:

$$H(\eta_1, \eta_2) = \frac{1}{2} \left[\frac{\pi}{4} \tan\left(\frac{\pi}{4}\eta_1\right) - \frac{\pi}{4} \cot\left(\frac{\pi}{4}\eta_2\right) + \frac{1}{\eta_2} \right]. \tag{B.5}$$

Now, if we recall the relationships $\eta_1 = (y + \bar{y})/g = \eta + \bar{\eta}$ and $\eta_2 = (y - \bar{y})/h = \eta - \bar{\eta}$, we obtain

$$H(\eta, \bar{\eta}) = \frac{1}{2} \left[\frac{1}{\eta - \bar{\eta}} - \frac{\pi}{2} \cdot \frac{\cos(\frac{\pi}{2}\eta)}{\sin(\frac{\pi}{2}\eta) - \sin(\frac{\pi}{2}\bar{\eta})} \right]. \quad (\text{B.6})$$

With the same reasoning as in Appendix A, the full linear approximation in η_2 is given by

$$H(\eta, \bar{\eta}) \simeq \frac{\pi}{8} \tan(\frac{\pi}{2}\bar{\eta}) + \epsilon_2(\bar{\eta})(\eta - \bar{\eta}), \quad (\text{B.7})$$

where $\epsilon_2(\bar{\eta})$ is defined in Eq. (52).

Appendix C. “The principle of electric images”

Throughout his long and fruitful scientific life, William Thomson (later Lord Kelvin) was in active correspondence with his father, the well known mathematician James Thomson, as well as with leading scientists in Great Britain and Europe. The topics of the letters were both personal and discussion of the latest scientific news and emerging new ideas. In addition, at the insistence of his father, W. Thomson kept diaries in mathematics and physics. These letters and diaries have been preserved and published [37,38], allowing us to trace the roots of ideas and the time of their origin.

As follows from the mathematical diary of 21-year-old W. Thomson [38], the story of “the principle of electric images” began in 1845, during his four-month stay in Paris. This trip abroad had several objectives. First, to improve the physical condition and also personally get acquainted with the leading French mathematicians (Liouville, Cauchy, Sturm), physicists (Arago, Biot, Pouillet), chemists (Regnault) and attend their lectures at the École Polytechnique and the Collège de France [38]. Before Thomson had been a month in Paris he sent to Liouville’s *Journal de Mathématiques* (vol. X. p. 137, 1845) a paper entitled “Démonstration d’un théorème d’analyse”, which two years later he expanded in the *Cambridge and Dublin Mathematical Journal* (vol. II. p. 109, March 1847) under the title: “On certain definite integrals suggested by problems in the theory of electricity”. This article allowed Thomson to demonstrate his skills as a mathematician and identified his area of interest as a natural philosopher.

During long conversations and discussions of the results of Faraday’s experiments and problems in the development of the mathematical theory of electricity, J. Liouville engaged W. Thomson to write a memoir for the Institute, with his vision of their solution [38]. Common interests in mathematics and physics made friends of Thomson and Liouville. Liouville’s friendship meant much to Thomson. To Liouville he confided his ideas about electric images.

From the mathematical diary ([38], p. 126): “March 15, 1845—I am occupied the whole day in Regnault’s physical laboratory at the Collège de France. At spare times I have been reading Poisson’s memoirs on electricity, which I find among the Memoirs of the Institute in Regnault’s cabinet. I have applied my ideas on induction in spheres and the principle of successive influence, and get a very simple solution, in the form Poisson gives it, for two spheres. I think I can work it out for i spheres ... The *image* of an exterior point, in a conducting sphere, is a p . in the interior, with opposite electr.”

In a footnote added in 1872 to one of his 1848 articles, Thomson describes this period as follows (Ref. [3], p. 52):

“...A complete exposition of the principle of electrical images (of which a short account was read at the late meeting of the British Association at Oxford) has not yet been published; but an outline of it was communicated by me to M. Liouville in three letters, of which extracts are published in the *Journal de Mathématiques* (1845 and 1847, vols. X., XII.). A full and

elegant exposition of the method indicated, together with some highly interesting applications to problems in geometry not contemplated by me, are given by M. Liouville himself, in an article written with reference to those letters, and published along with the last of them. I cannot neglect the present opportunity of expressing my thanks for the honour which has thus been conferred upon me by so distinguished a mathematician, as well as for the kind manner in which he received those communications, imperfect as they were, and for the favourable mention made of them in his own valuable memoir.”

Thomson does not seem to have made the acquaintance of G. G. Stokes till after his return from Paris in May 1845; at least Stokes’s name never occurs in Thomson’s earlier letters or in his diary. Yet he was settled in Pembroke as a junior fellow, having been Senior Wrangler in 1841. It seems that it was the task of editing the *Cambridge and Dublin Mathematical Journal* that brought them together; and Stokes’s penchant for experimenting led Thomson often to seek his advice. Stokes was indeed guide, philosopher, and friend to his eager and enthusiastic disciple. Many years later Lord Kelvin said (Ref. [39], p. 318): “For sixty years of my own life, from 1843 to 1903, I looked up to Stokes as my teacher, guide, and friend.” For more than fifty years (1846–1903) each was in the habit of communicating to the other the progress of his ideas.

On June 20, 1847, Thomson writes from Peterhouse to his father about the approaching meeting of the British Association (Ref. [38], p. 204): “...I have been getting out various interesting pieces of work, along with Stokes, connected with some problems in electricity, fluid motion, etc., that I have been thinking on for years, and I am now seeing my way better than I could ever have done by myself, or with any other person than Stokes.”

In July 1847, Thomson and Stokes attended the meeting of the British Association at Oxford with talks entitled “On Electrical Images” (by W. Thomson) and “On the Resistance of a Fluid to two Oscillating Spheres” (by G. G. Stokes). One year later the Report of the Seventeenth Meeting of the British Association was published; however, the results of Thomson and Stokes were presented by short abstracts. Some extracts from these abstracts follow.

W. Thomson [2]:

“There is no branch of natural philosophy of which the elementary laws are more simple than those which regulate the distribution of electricity upon conducting bodies; yet its impracticability has always been the reproach of the mathematical theory of electricity. Very few of the varied and interesting problems which it presents have been made subjects for investigation, on account of the apparently extreme complexity of the conditions to be satisfied; and even when results have been forced from it by the analytical skill and energy of a Poisson, the physical interest has been almost lost in the struggle with mathematical difficulties, and the complexity of the solution has eluded that full interpretation without which the mind cannot be satisfied in any analytical operations having for their object the investigation or expression of truth in natural philosophy ...

The subject of this communication is ‘the principle of electrical images,’ which is suggested by Green’s elementary propositions, as the proper way of treating a great variety of problems that present themselves with reference to the distribution of electricity on spherical conductors. The effect of a body electrified in any given manner upon an uninsulated sphere is shown to be completely represented by what may be called ‘the image of the electrified body in the sphere,’ and a simple geometrical construction is given by which this image may be described. When an electrified body is placed in the neighbourhood of two uninsulated spheres, an inductive

effect is produced which may be represented by an infinite series of ‘successive images’ in each sphere. An algebraic expression of this result leads to solutions, by means of converging series, of the various problems which occur with reference to the distribution of the induced electricity, and the attractions exerted by the two spheres. When a single conductor bounded by segments of two spherical surfaces cutting at an angle which is a submultiple of two right angles is electrified by the influence of a charged body, the effect may be represented by means of a finite number of images disposed in a symmetrical manner in the circumference of a circle passing through the exciting body, and cutting the two spherical surfaces at right angles. The principle of electrical images, as applied in these two cases, may be illustrated by a reference to the successive images of a candle placed between two parallel plane mirrors, and to the symmetrically arranged images which are seen in the kaleidoscope.”

G. G. Stokes [4]:

“The object of this communication was to shew the application of Professor Thomson’s method of images to the solution of certain problems in hydrodynamics ...

The investigation mentioned in the preceding paper arose out of the communication to me by Sir William Thomson of his beautiful method of electrical images before he had published it. Having myself paid more attention to the motion of fluids than to electricity, I endeavoured to find if it would in any manner apply to the solution of problems in the motion of fluids. I found that what is called above a singular point of the second order¹⁰ had a perfect image in a sphere when its axis was in the direction of a radius, which led to a complete solution of the problem mentioned in the paper when one sphere lay wholly outside or inside the other.”

Many years later, an extended version of this report was published in Ref. [40]. After this article, the method of images became one of the problem-solving techniques in hydrodynamics [5,6].

It should be noted that the technique of electrical images is described by Thomson fragmentary and scattered across articles of different years. The most consistent presentation of this method with use of the idea of the potential and of equipotential surfaces is given in “A Treatise on Electricity and Magnetism” by Maxwell [21]. This is how Maxwell begins to introduce the reader to the principle of image charges:

“...In applying this method to the most elementary case of a sphere under the influence of a single electrified point, we require to expand the potential due to the electrified point in a series of solid harmonics, and to determine a second series of solid harmonics which express the potential, due to the electrification of the sphere, in the space outside. It does not appear that any of these mathematicians observed that this second series expresses the potential due to an imaginary electrified point, which has no physical existence as an electrified point, but which may be called an electrical image, because the action of the surface on external points is the same as that which would be produced by the imaginary electrified point if the spherical surface were removed.

This discovery seems to have been reserved for Sir W. Thomson, who has developed it into a method of great power for the solution of electrical problems, and at the same time capable of being presented in an elementary geometrical form ...” [21]

¹⁰ Currently called a doublet or dipole.

Thus, the method of image charges and currents allows us to solve problems on the distribution of real charges and fields not only due to the conductive surface of the simplest geometric form, a plane, but also for conductors of more complex geometric shapes.

References

- [1] W. Thomson, *J. Math. Pure. Appl.* **X**, 364 (1845).
- [2] W. Thomson, On electrical images, in *Report of the Seventeenth Meeting of the British Association for the Advancement of Science* (John Murray, London, 1848), Vol. 1, Part II, p. 6.
- [3] W. Thomson, *Reprint of Papers on Electrostatics and Magnetism* (Macmillan, London, 1884), 2nd ed., Vol. 1, p. 144.
- [4] G. G. Stokes, On the resistance of a fluid to two oscillating spheres, in *Report of the Seventeenth Meeting of the British Association for the Advancement of Science* (John Murray, London, 1848), Vol. 1, Part II, p. 6.
- [5] H. Lamb, *Hydrodynamics* (Cambridge University Press, Cambridge, UK, 1932), 6th ed.
- [6] J. N. Newman, *Marine Hydrodynamics* (MIT Press, Cambridge, MA, 1999).
- [7] L. J. Laslett, Proc. BNL Summer Study on Storage Rings, BNL-7534, p. 324 (1963).
- [8] L. J. Laslett, *Selected Works of L. Jackson Laslett* (Lawrence Berkeley Laboratory, Berkeley, 1987), LBL-PUB-616, Vol. 3.
- [9] R. Cimino, I. R. Collins, M. A. Furman, M. Pivi, F. Ruggiero, G. Rumolo, and F. Zimmermann, *Phys. Rev. Lett.* **93**, 014801 (2004).
- [10] B. B. Levchenko, [arXiv:physics/0608135](https://arxiv.org/abs/physics/0608135)[physics.acc-ph] [[Search INSPIRE](#)].
- [11] B. Levchenko, *Phys. Res. Int.* **2010**, 201730 (2010).
- [12] M. Sands, *The Physics of Electron Storage Rings: An Introduction* (Stanford Linear Accelerator Center, Menlo Park, 1970), SLAC-0121.
- [13] H. Wiedemann, *Particle Accelerator Physics* (Springer, Berlin, 2007).
- [14] A. W. Chao, *Physics of Collective Beam Instabilities in High-Energy Accelerators* (Wiley, New York, 1993).
- [15] I. N. Bronshtein and K. A. Semendyayev, *A Guide Book to Mathematics* (Springer, New York, 1973).
- [16] M. Ferrario, V. Fusco, and M. Migliorati, Electric field for a uniformly charged cylindrical bunch with elliptical cross section, *Technical Report SPARC-BD-03/002* (Istituto Nazionale di Fisica Nucleare, Frascati, 2003).
- [17] W.-M. Yao et al. [Particle Data Group], *J. Phys. G: Nucl. Part. Phys.* **33**, 1 (2006).
- [18] M. A. Furman, *Am. J. Phys.* **62**, 1134 (1994).
- [19] M. A. Furman, Compact complex expressions for the electric field of 2D elliptical charge distributions (with corrections and additions) (Lawrence Berkeley Laboratory, Berkeley, 2007) (available at: <http://mafurman.lbl.gov/mafurman.lbl.gov/LBL-34682.pdf>).
- [20] M. Altarelli, R. Brinkmann, M. Chergui et al. (eds.), XFEL: The European X-Ray Free-Electron Laser. *Technical Design Report DESY-06-097*. (DESY, Hamburg, 2006).
- [21] J. C. Maxwell, *A Treatise on Electricity and Magnetism* (Oxford University Press, Oxford, UK, 1873), Vol. 1, Chap. 11.
- [22] A. Hofmann, in: "Jyvaeskylae 1992, Proceedings, General accelerator physics, vol. 1," CERN Geneva, CERN-94-01 (94/01, rec. Mar.) 329-348 (1992).
- [23] B. Zotter, Coherent Q-shift of a relativistic particle beam in a metallic vacuum chamber, *Technical Report CERN-ISR-TH/72-8* (CERN, Geneva, 1972).
- [24] S. Petracca, *Part. Acc.* **62**, 241 (1999).
- [25] B. Zotter, Space charge effects in circular accelerators, in *Handbook of Accelerator Physics and Engineering*, eds. A. Wu Chao and M. Tigner (World Scientific, Singapore, 1999), p. 112.
- [26] O. Brüning, P. Collier, P. Lebrun et al. (eds.), *LHC Design Report: The LHC Main Ring* (CERN, Geneva, 2004), Vol. 1.
- [27] G. Apollinari, I. Béjar Alonso, O. Brüning et al. (eds.), *High-Luminosity Large Hadron Collider (HL-LHC)* (CERN, Geneva, 2017), Volume 1.
- [28] P. Pashkov, *Beam Physics in Circular Accelerators* (Fizmatlit, Moscow, 2006) [in Russian].
- [29] M. Reiser, *Theory and Design of Charged Particle Beams* (Wiley, Weinheim, 2008).
- [30] B. B. Levchenko, [arXiv:1810.12109v1](https://arxiv.org/abs/1810.12109v1) [physics.acc-ph] [[Search INSPIRE](#)].
- [31] W. R. Smythe, *Static and Dynamic Electricity* (McGraw-Hill, New York, 1950).

- [32] B. Zotter, Nucl. Instrum. Meth. **129**, 377 (1975).
- [33] K. Y. Ng, Betatron tune shifts and Laslett image coefficients *Technical Report FERMILAB-TM-2152* (Fermilab, Batavia, 2001).
- [34] S. Petracca, Part. Acc. **49**, 181 (1994).
- [35] CERN Courier, **59**, 9 (2019) (available at: <https://cerncourier.com/a/report-reveals-full-reach-of-lhc-programme/>, date last accessed January 2, 2020).
- [36] I. S. Gradshteyn and I. M. Ryzhik, *Table of Integrals, Series, and Products* (Academic, New York, 1980).
- [37] D. B. Wilson (ed.), *The Correspondence between Sir George Gabriel Stokes and Sir William Thomson, Baron Kelvin of Largs* (Cambridge University Press, Cambridge, UK, 1990), Vols. 1 and 2.
- [38] S. P. Thompson, *The Life of William Thomson, Baron Kelvin of Largs* (Macmillan, London, 1910), Vol. 1 and Vol. 2.
- [39] J. Larmor (ed.), *Memoir and Scientific Correspondence of the Late Sir George Gabriel Stokes, Bart.* (Cambridge University Press, Cambridge, UK, 1907), Vol. 1.
- [40] G. G. Stokes, *Mathematical and Physical Papers* (Cambridge University Press, Cambridge, UK, 1880), Vol. 1, p. 230.